

SNIa in the NIR, MIR & beyond

(P. Hoeflich, FSU & 1/3 of the audience)

1) Why, what physics and the diversity ?



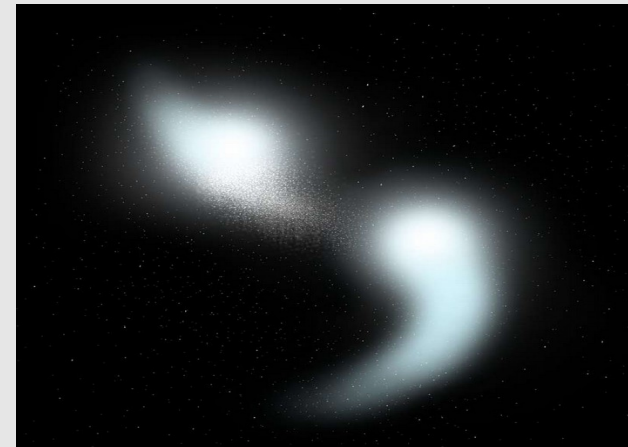
R.Hines

2) Early time NIR spectra

3) Late time NIR

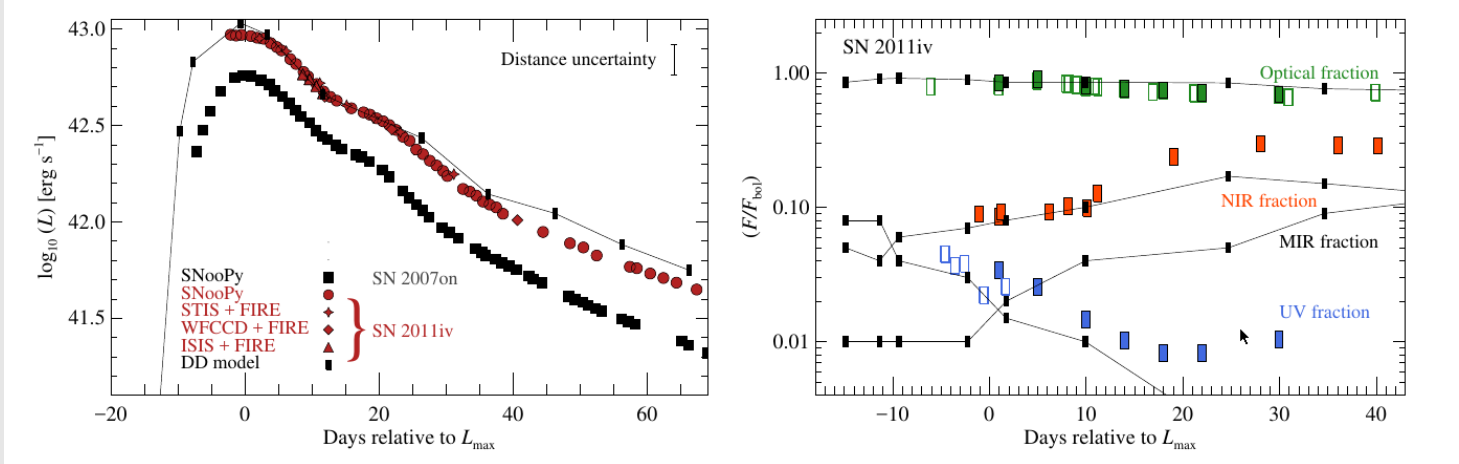
4) Ultra-late times

5) Summary & wishlist



Why do we need NIR and MIR

- Energy redistribution in LC & SNIa cosmology (Example from Gall et al. 2017)

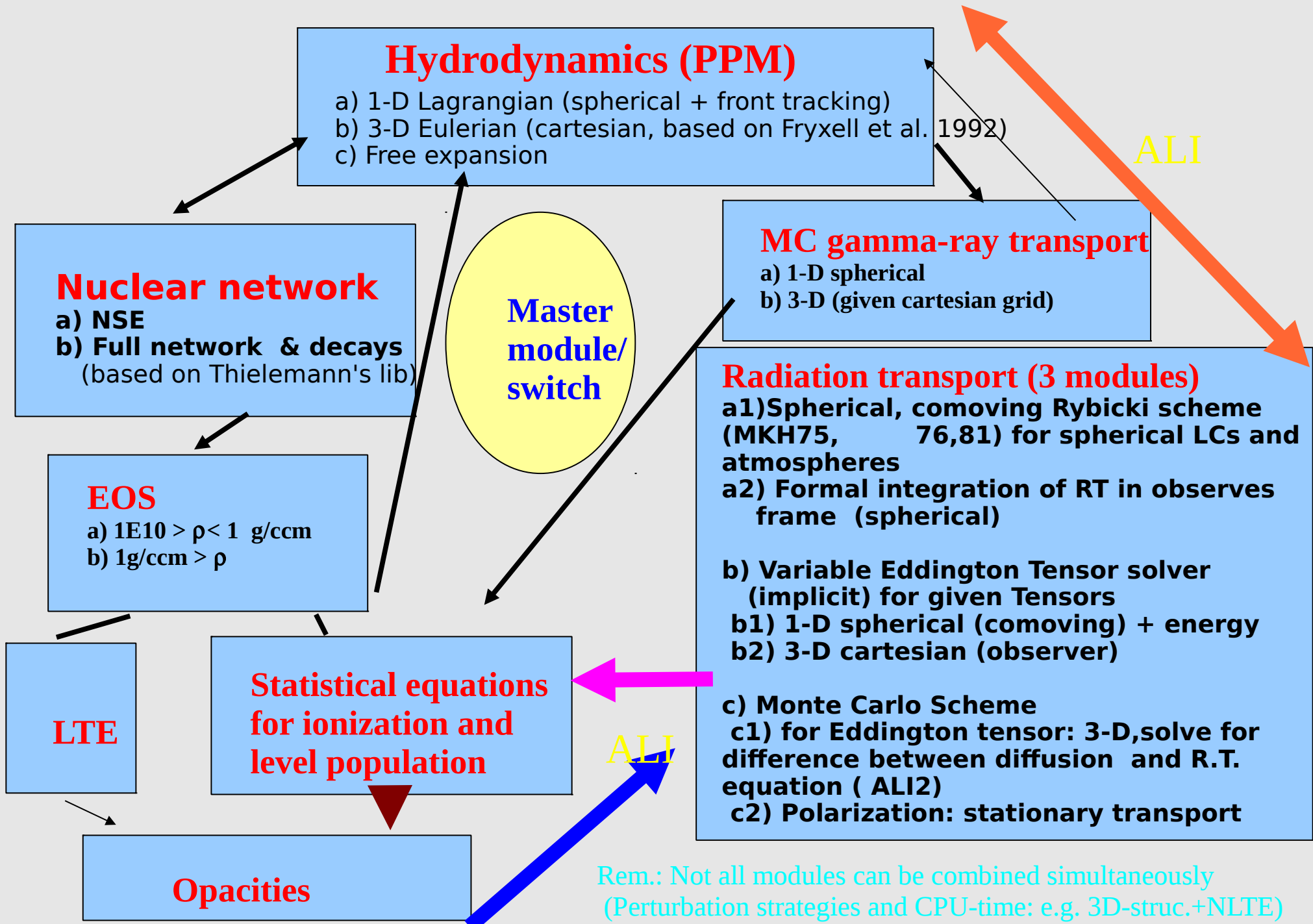


SN 2007on/11iv
& models

- Probe of key elements and ions without suitable lines in optical (Ar, Ne, ^{57}Co)
- Line profiles of hardly blended features → 3D structure of elements
→ directional dependence
- Molecules and dust → Environment

Remark: Models are useful to identify problems, tell-tails and quantitative analyses
Problem: Huge parameter space

Numerical Environment of *HYD*_{hydrodynamical} *RA*_{radiation} transport



Some characteristics of results shown

- Non-LTE LCs and Spectra in spherical & 2D, 3D geometry (Hoeflich 2002, Hoeflich et al. 2017, and refs.)
- Gamma- & positron transport by Monte Carlo (Penny & Hoeflich, 2015)
- Time-dependent ionization balance (Hoeflich 1993, 1995)

Some Technical Details (and why):

- Momentum equation (VLT) to couple flux & energy equation & hydra in multi-group with Rybicki-scheme (MKH) and MC in spherical and 3D, respectively

with

$$S_\nu = \frac{\eta_\nu}{\chi_\nu} \quad (III.2.11)$$
$$\eta_\nu = \frac{2h\nu^3}{c^2} \sum_{element} \sum_{ion} \left[\sum_{i=1}^I \left[n_i^* \alpha_{ik}(\nu) e^{-\frac{h\nu}{kT}} + \sum_{j>i}^I (\alpha_{ij}(\nu) n_j \frac{g_i}{g_j}) \right] + n_e n_{ion} \alpha_{ff}(\nu) e^{-h\nu/kT} \right] + \left[n_e \sigma_e + \sum_{scat.lines} \chi_l \right] J_\nu \quad (III.2.12)$$

and

$$\chi_\nu = \sum_{element} \sum_{ion} \left[\sum_{i=1}^I \left[\alpha_{ik}(\nu) \left(n_i - n_i^* e^{-\frac{h\nu}{kT}} \right) + \sum_{j>i}^I \alpha_{ij}(\nu) \left(n_i - n_j \frac{g_i}{g_j} \right) \right] + n_e n_{ion} \alpha_{ff}(\nu) (1 - e^{-\frac{h\nu}{kT}}) \right] + \left[n_e \sigma_e + \sum_{scat.lines} \chi_l \right] \quad (III.2.13)$$

Some Technical Details II (and why):

- Non-LTE solution is converged **iteratively by double-loops**
 - a) Accelerated Lambda-Iteration for each transition (**to drive convergence of specific transitions**).
 - b) **Iteration** using equivalent-two level scheme to include non-local coupling in radiation transport
- to drive non-local coupling in frequency space and between elements and ions.
- **Rem.: Avoids instabilities during the temperature iteration** (using net-heating rates and ALI, Hubeny) case of in high depth resolution.

$$\bar{S}_{lu} = \frac{(\int \phi_\nu J_\nu + (\varepsilon' + \theta) B_\nu)}{(1 + \varepsilon' + \varsigma)} \quad (III.2.25)$$

with

$$\int \phi_\nu d\nu = 1 \quad (III.2.26)$$

23

one gets

$$\varsigma = \frac{(a_2 a_3 - \frac{g_l}{g_u} a_1 a_4)}{(A_{ul}(a_2 + a_4))} \quad (III.2.27)$$

$$\theta = \frac{n_1^* a_1 a_4 (1 - e^{-h\nu/kT})}{(A_{ul} n_u^* (a_2 + a_4))} \quad (III.2.28)$$

$$\varepsilon' = C_{ul} (1 - e^{-h\nu/kT}) / A_{ul} \quad (III.2.29)$$

with

$$a_1 = R_{lk} + C_{lk} + \sum_{i < l} \frac{n_i^*}{n_l^*} R_{li} - \frac{n_i}{n_l} R_{il} + \sum_{l < j \neq u} \left(1 - \frac{b_j}{b_l}\right) C_{lj} \quad (III.2.30)$$

$$a_2 = n_l^* (R_{kl} + C_{lk}) + \sum_{l < j \neq u} b_j n_l^* R_{jl} - n_l R_{lj} + \sum_{i < l} n_i C_{il} \left(1 - \frac{b_l}{b_i}\right) \quad (III.2.31)$$

$$a_3 = R_{uk} + C_{uk} + \sum_{u > i \neq l} \frac{n_i^*}{n_u^*} R_{ui} - \frac{n_i}{n_u} R_{iu} + \sum_{u > i} \left(1 - \frac{b_j}{b_u}\right) C_{uj} \quad (III.2.31b)$$

$$a_4 = n_u^* (R_{ku} + C_{uk}) + \sum_{u < j} b_j n_u^* R_{ju} - n_u R_{uj} + \sum_{u > i \neq l} n_i C_{iu} \left(1 - \frac{b_u}{b_i}\right). \quad (III.2.32)$$

- c) **Iteration** of partial-redistribution source function because **overlapping lines in co-moving frame**

Some Technical Details III (and why):

- c) Implicit time-dependence in non-LTE to avoid Courant-Hilbert condition for hydro-time step.

In general, the time dependent rate equations are given by the expression

$$\frac{\partial n_i}{\partial t} + \nabla(n_i v) = \sum_{i \neq j} (n_j P_{ji} - n_i P_{ij}) + n_k (R_{ki} + C_{ki}) - n_i (R_{ik} + C_{ik}) \quad (B1)$$

↗

If we subtract the time-independent solution \tilde{n} and

$$\frac{\partial n_i}{\partial t} + \frac{\partial}{\partial r}(n_i v(r)) = n_k (R_{ki} + C_{ki}) - \frac{\tilde{n}_k}{\tilde{n}_i} (R_{ki} + C_{ki}) n_i \quad (B5)$$

i.e. an inhomogeneous linear differential equation of first order

$$\Rightarrow \frac{dn_i}{dt} = -C_1 n_i + C_2 \quad (B6)$$

with

$$C_1 := \frac{\tilde{n}_k}{\tilde{n}_i} (R_{ki} + C_{ki}) \quad (B7)$$
$$C_2 := n_k (R_{ki} + C_{ki})$$

Thumbnail Sketch of Thermonuclear Supernovae

SNe Ia are **thermonuclear** explosions of White Dwarfs (C/O core of a star with less than $8 M_{\odot}$)

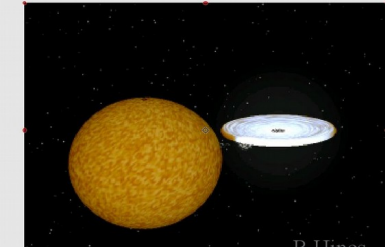
SNe Ia are homogeneous because **nuclear physics** determines the WD structure & explosion
The total energy production is given by the total amount of burning
The light curves are determined by the amount of radioactive ^{56}Ni

Classes of Progenitor Systems

Accreting WD (MS, RG, He-star, C-star) (SD-systems)

(e.g. Nomoto et al. 1984, Wang & Han, 2013), ...)

Two merging WDs (DD-systems)



R.Hines



Common Causes Diversity:

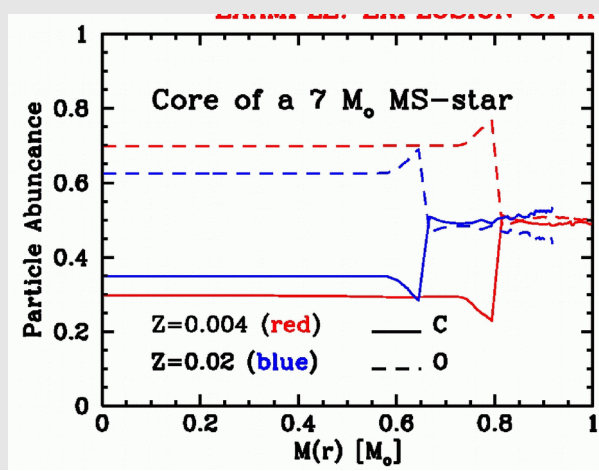
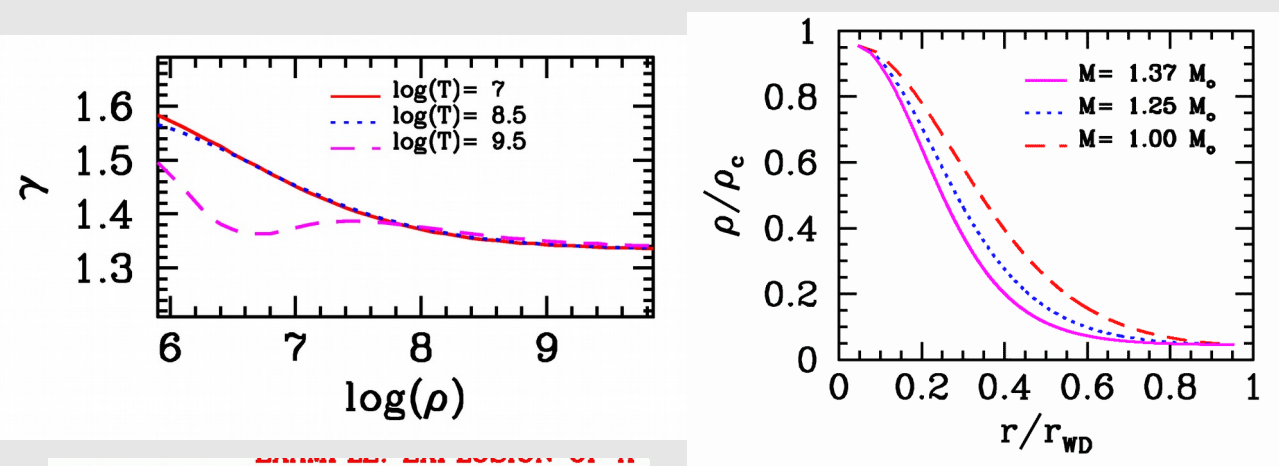
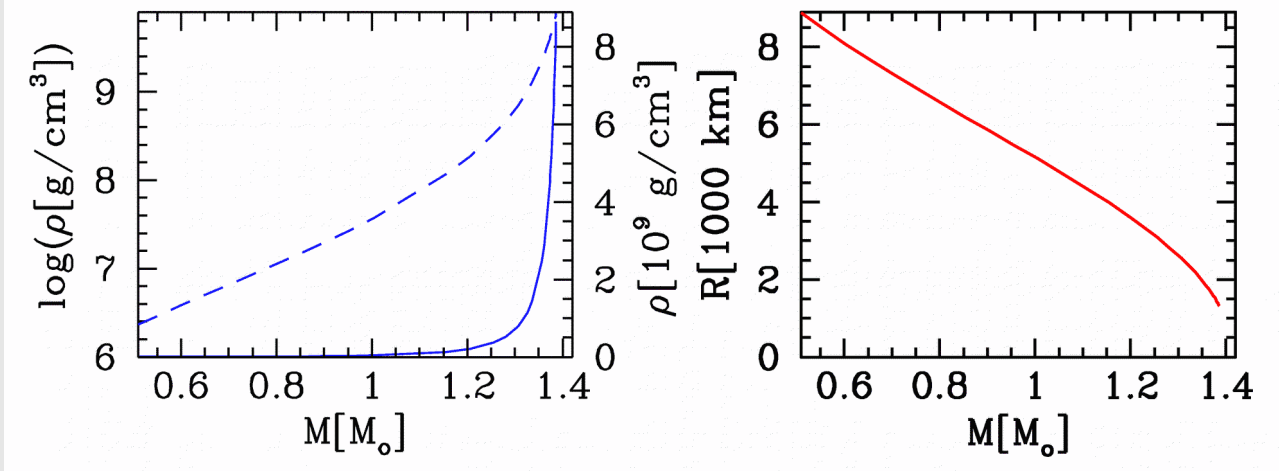
- Main Sequence mass M(MS) → Explosion energy E(nuc)
- Mass of progenitor → central density
- Metallicity Z → E(nuc) and ^{56}Ni
- Magnetic fields → Hydro & Spectra
- Environment → Interaction, 'ISM'

Classes for Explosions (see Kromer & Wang)

M(Ch) mass WDs: Ignition by compressional heat (originates from either SD or DD, CD)

Heat release during dynamic process (dynamical mergers, violent mergers, He-detonations)

Initial WD Structure or the Devil is in the Details



Dominguez et al. 2001
Hetal 2001

I) M(WD) influences

- $R(\text{WD})$
- $\rho(\text{c})$

Dividing line:

$M_{\text{Ch}} > 1.3 M_\odot$ (start as deflagration)
 $\text{Sub-}M_{\text{Ch}} < 1.2 M_\odot$ (“ “ detonation)

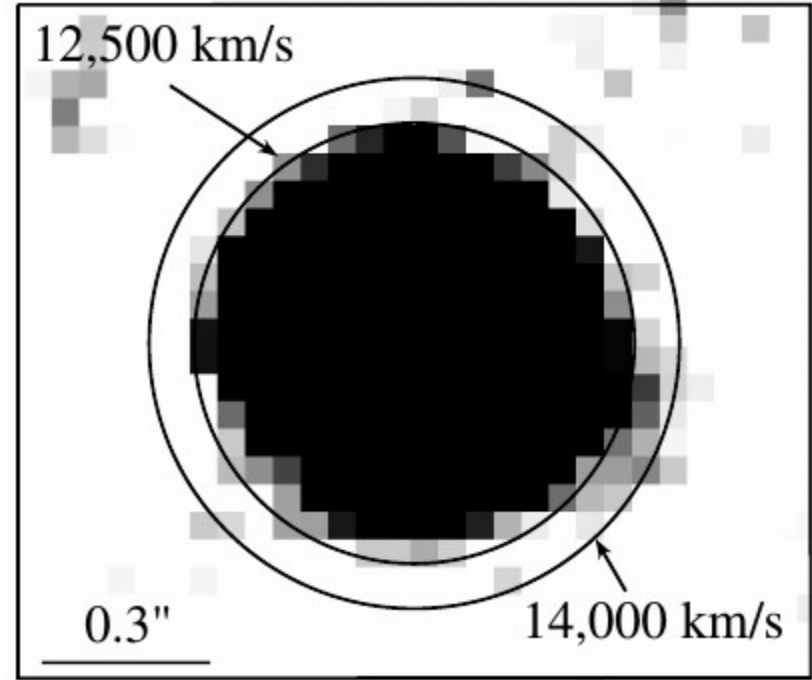
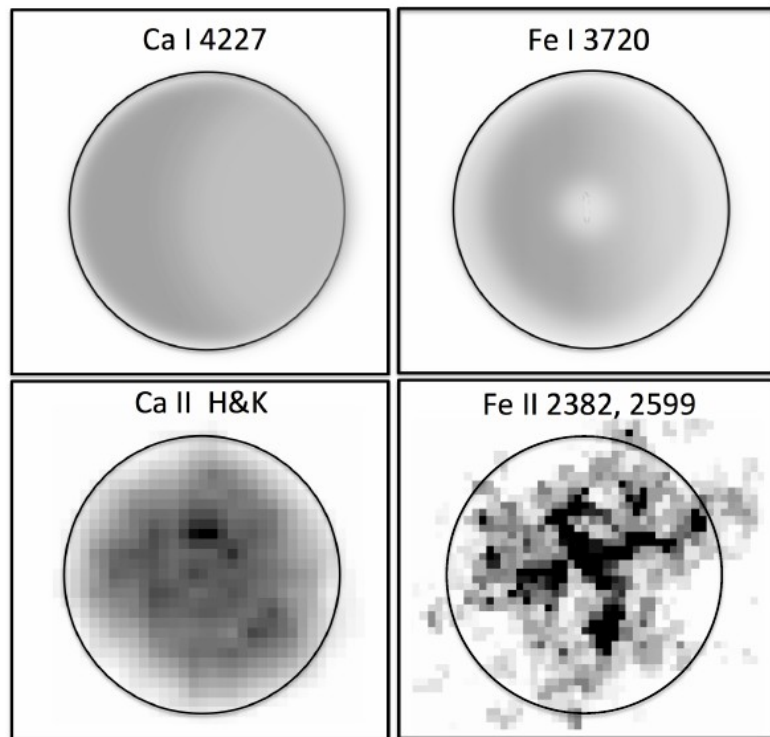
Rem: $M(\text{Ch}) \rightarrow$ partially relativistic EOS
 \Rightarrow density structure

II) M(MS) & Z changes

abundance structure
 \Rightarrow Nuclear energy release

& Multi-Dimensional:

Example: SN1885 with HST (Fesen et al. 2005,15,17)



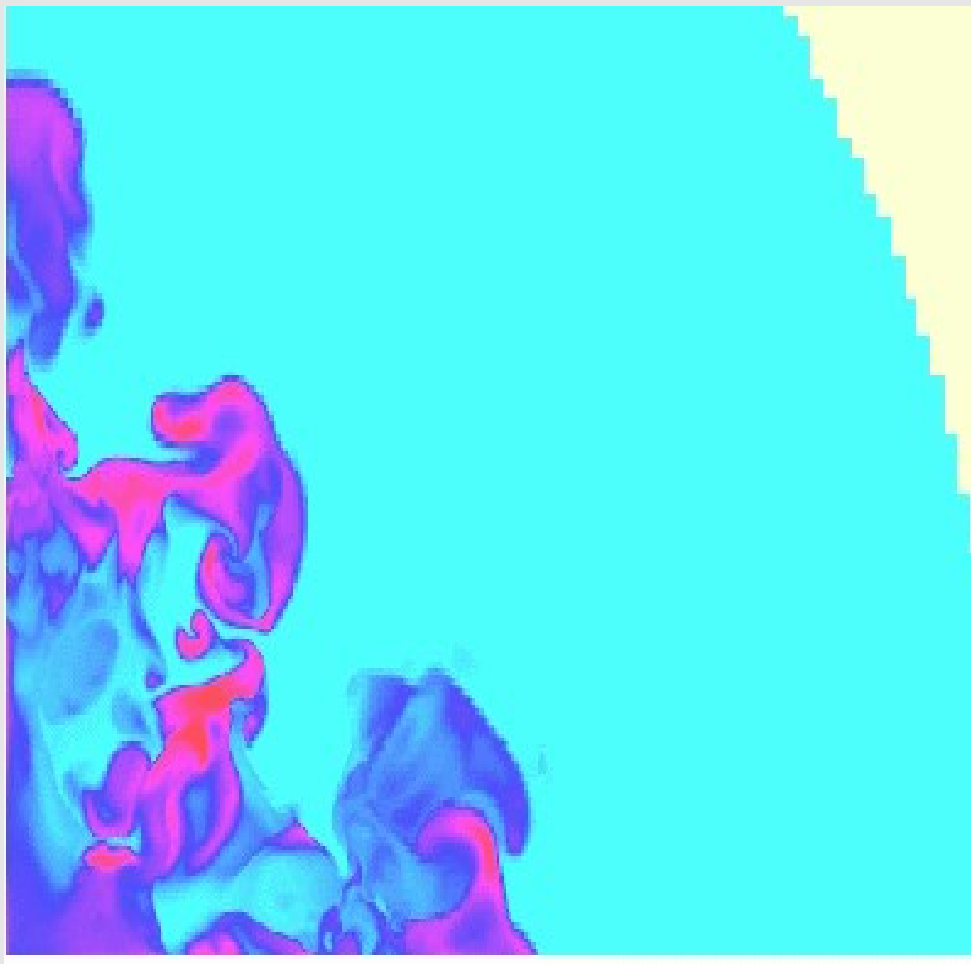
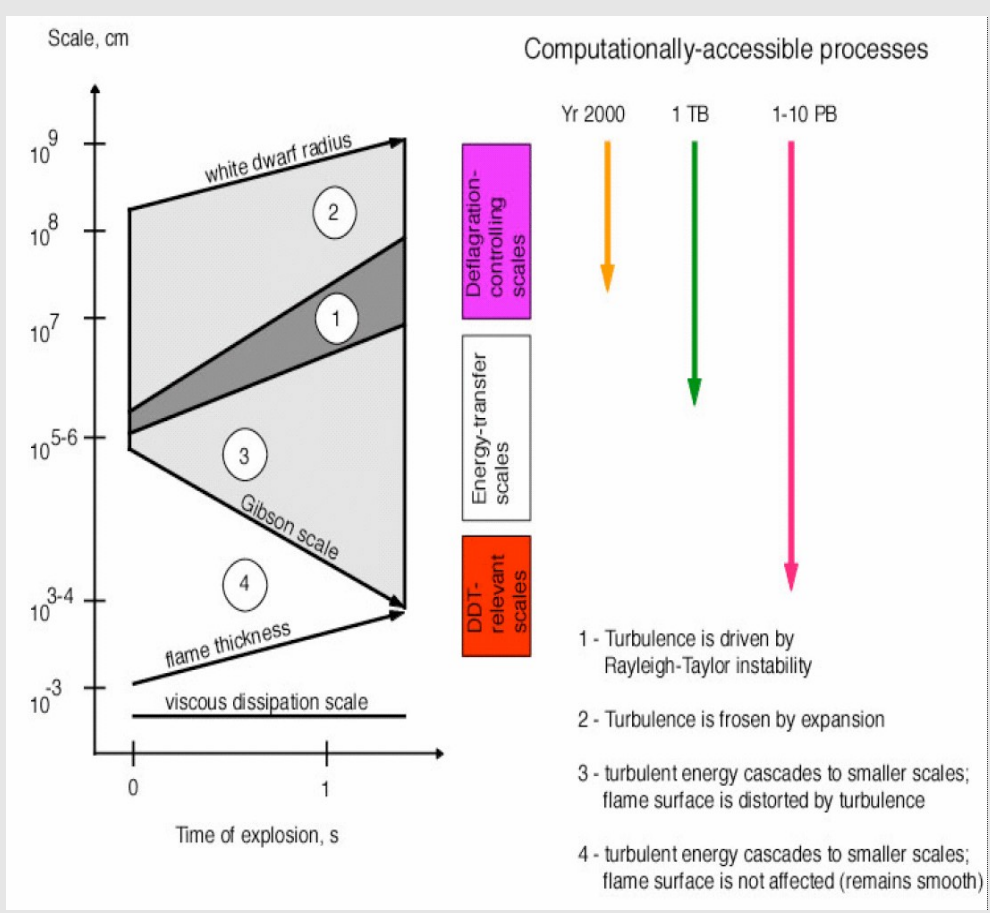
- Signature of deflagration fronts with reduced mixing
(Lucky case but hardly repeatable)

How can we get this information otherwise?

General Rule: Never look to close

Hydrodynamics of Nuclear Burning Fronts (Gamezo et al. 2003)

see also (Khokhlov et al. 2001, Niemeyer et al. 2002, Gamezo et al. 2004, Livne et al. 2003, Roepke et al. 2003, Hoeflich et al., 2004, Roepke et al. 2006/7, Fesen et al. 2007, ..., Seitenzahl et al. 2013)

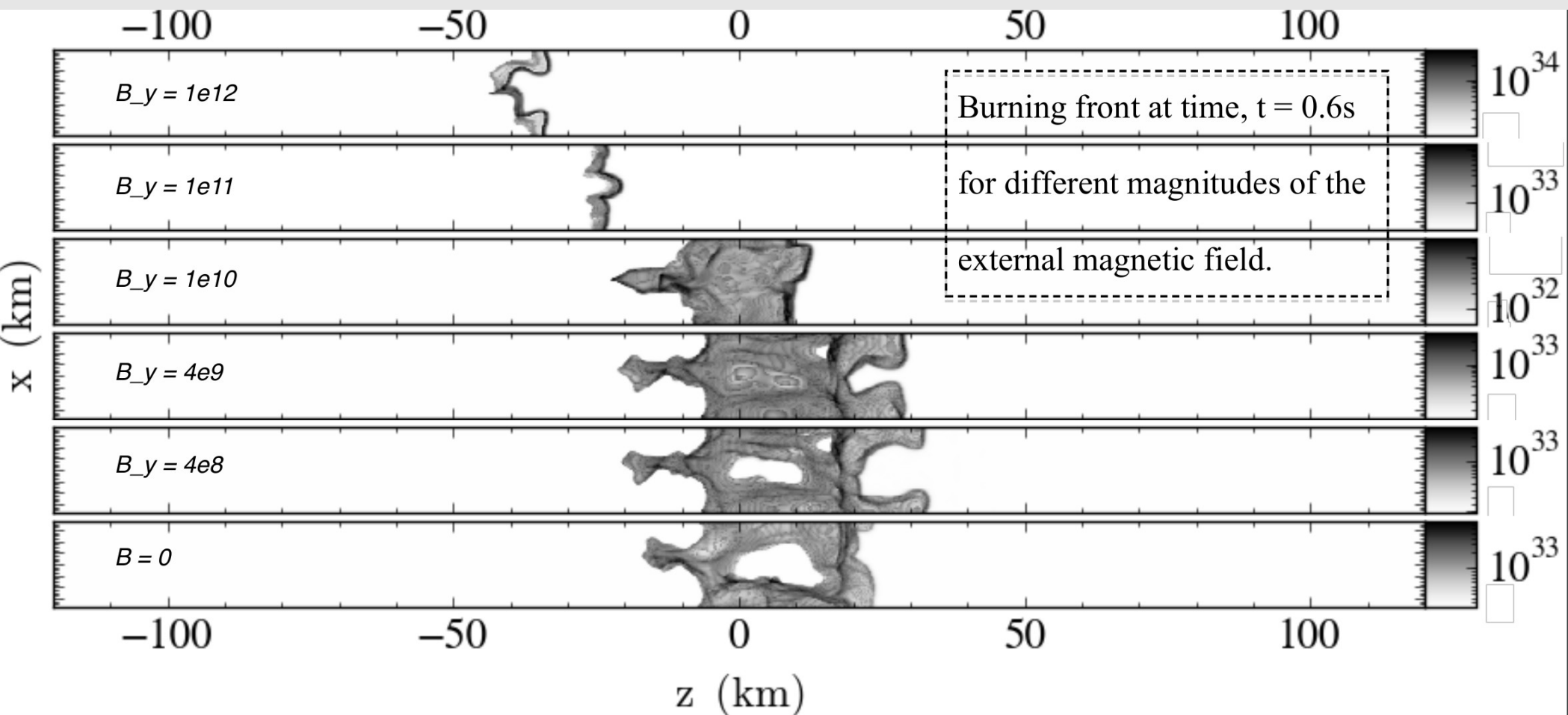


Problem: We do not see this kind of mixing !!!
Question: Shall we give up on M(Ch) ?

Influence of the B field no nulcear burning under WD conditions with ENZO

(B. Hiskov et al. 2014/16/17, see also Remming et al. 2015)

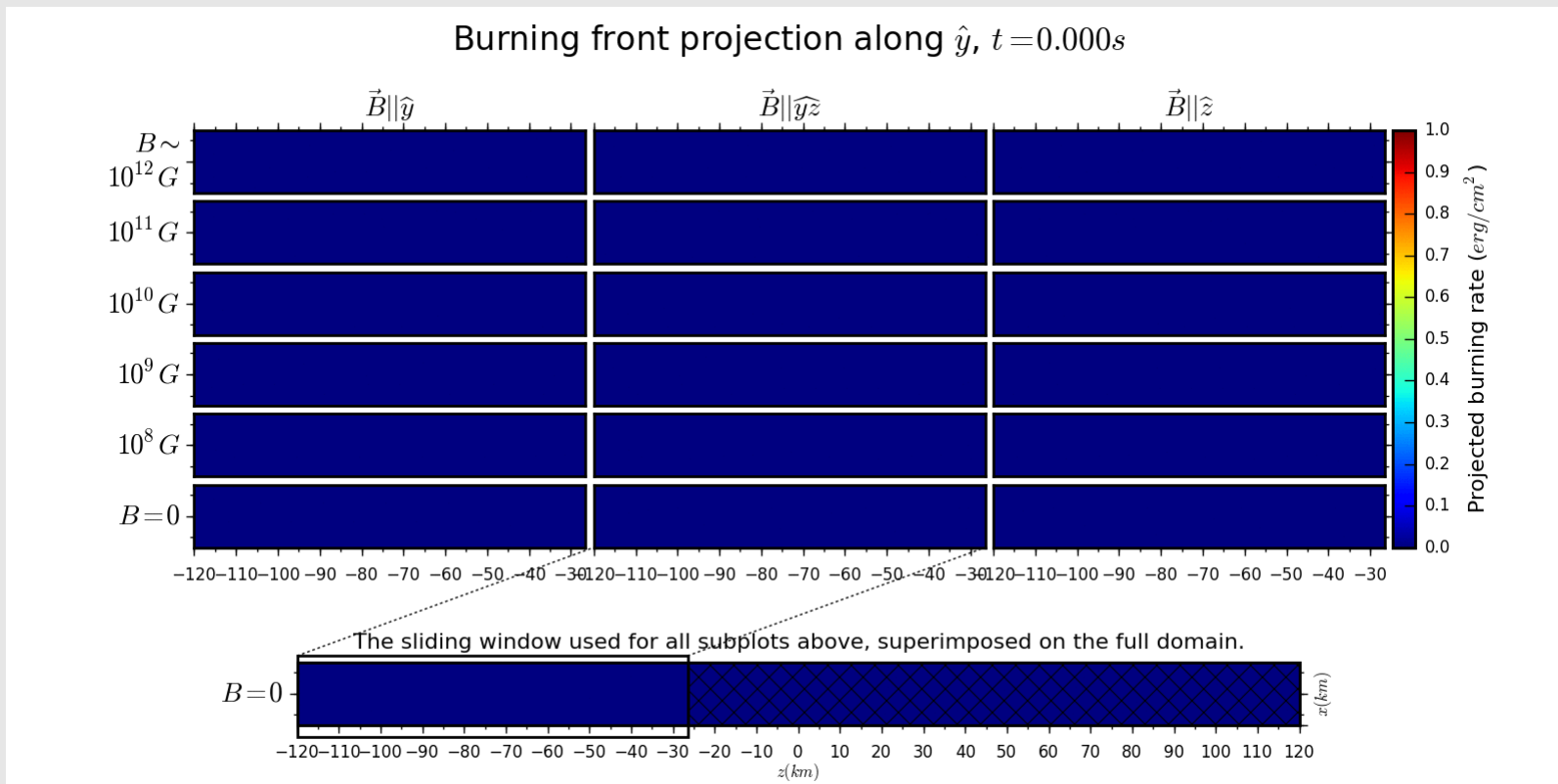
$\rho(1E8\text{g/ccm})$, C/O=1, $\gamma=1.35$, dE/dt)



Influence of the B field no nulcear burning under WD conditions with ENZO

(B. Hiskov, D. Collins, P. Hoeflich, 2015/16/17, see also Remming & Khokhlov, 2015)

$\rho(1E8 \text{ g/ccm})$, C/O=1, $\gamma=1.35$, dE/dt)

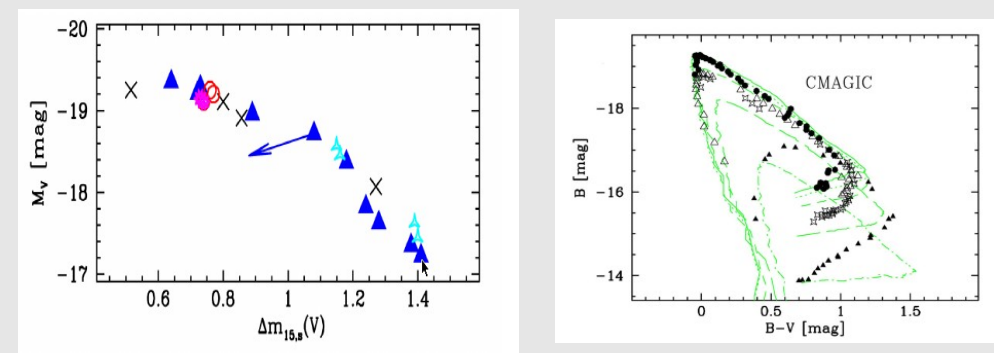
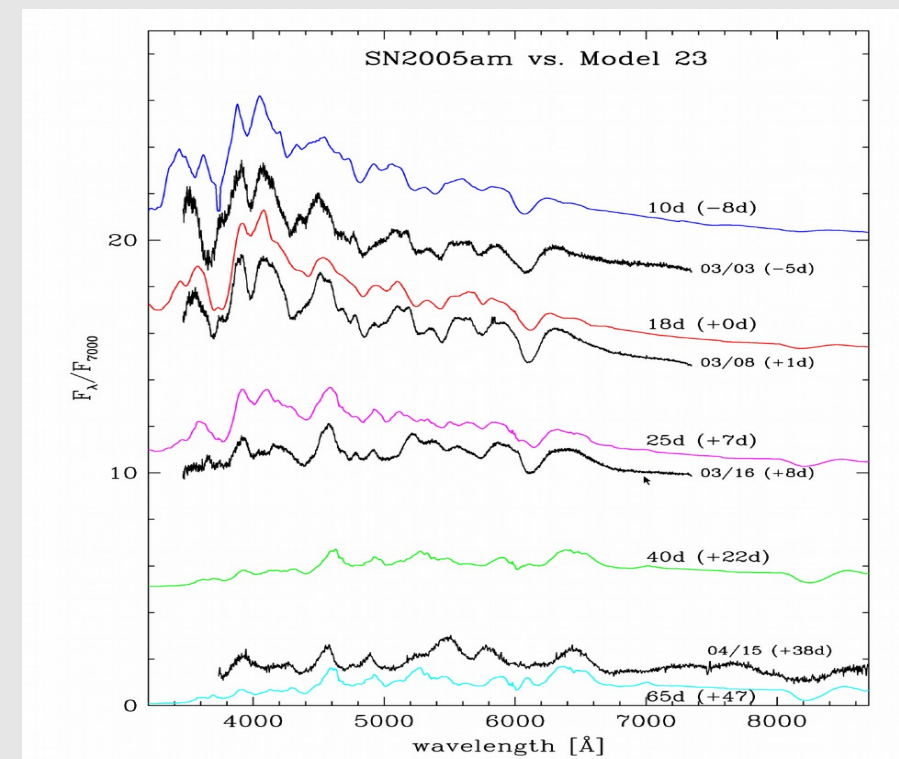
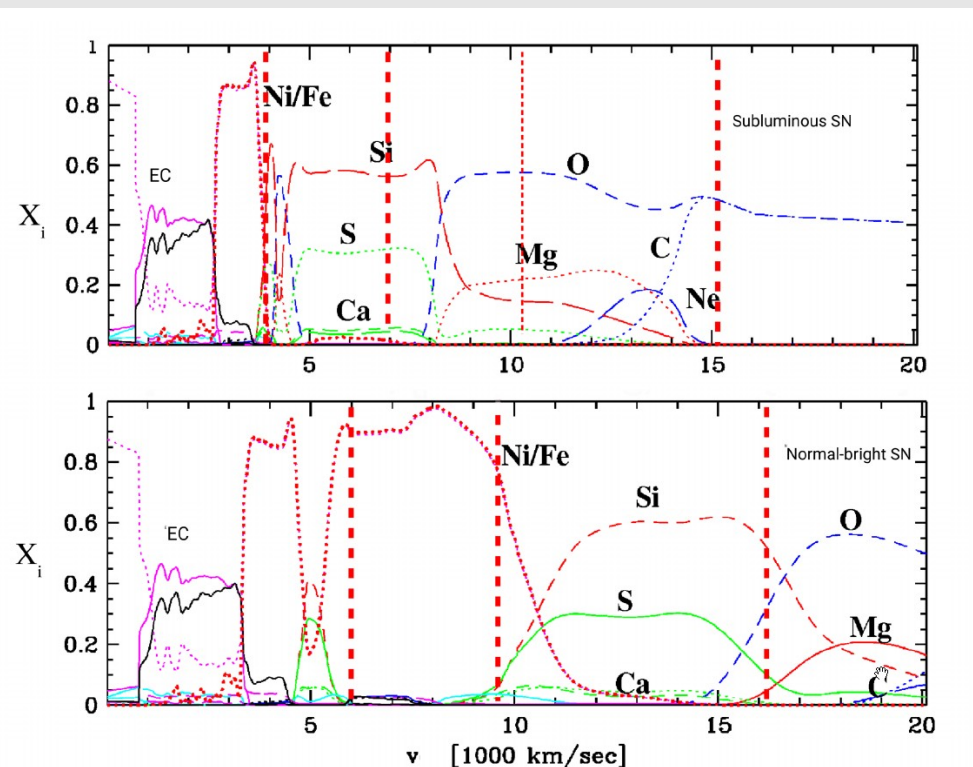
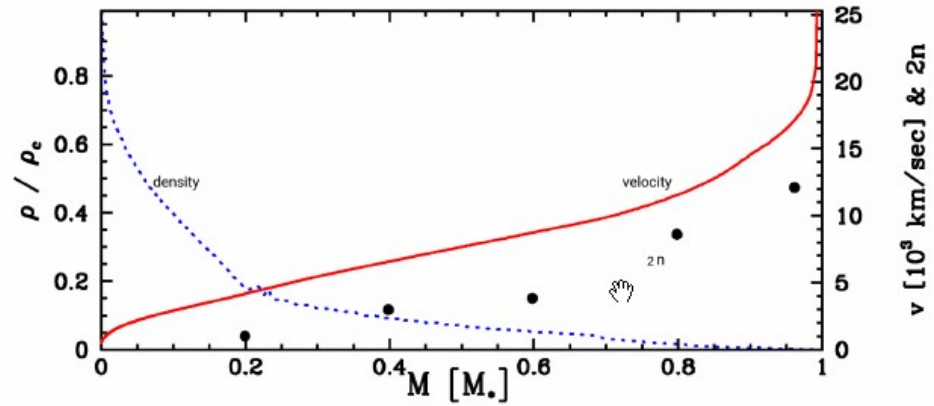


- High B fields slow down the burning front
- RT-instabilities are suppressed
- Coam-instabilities are created for high B.

Question: Does this cure the RT in SN models and create DDT ?

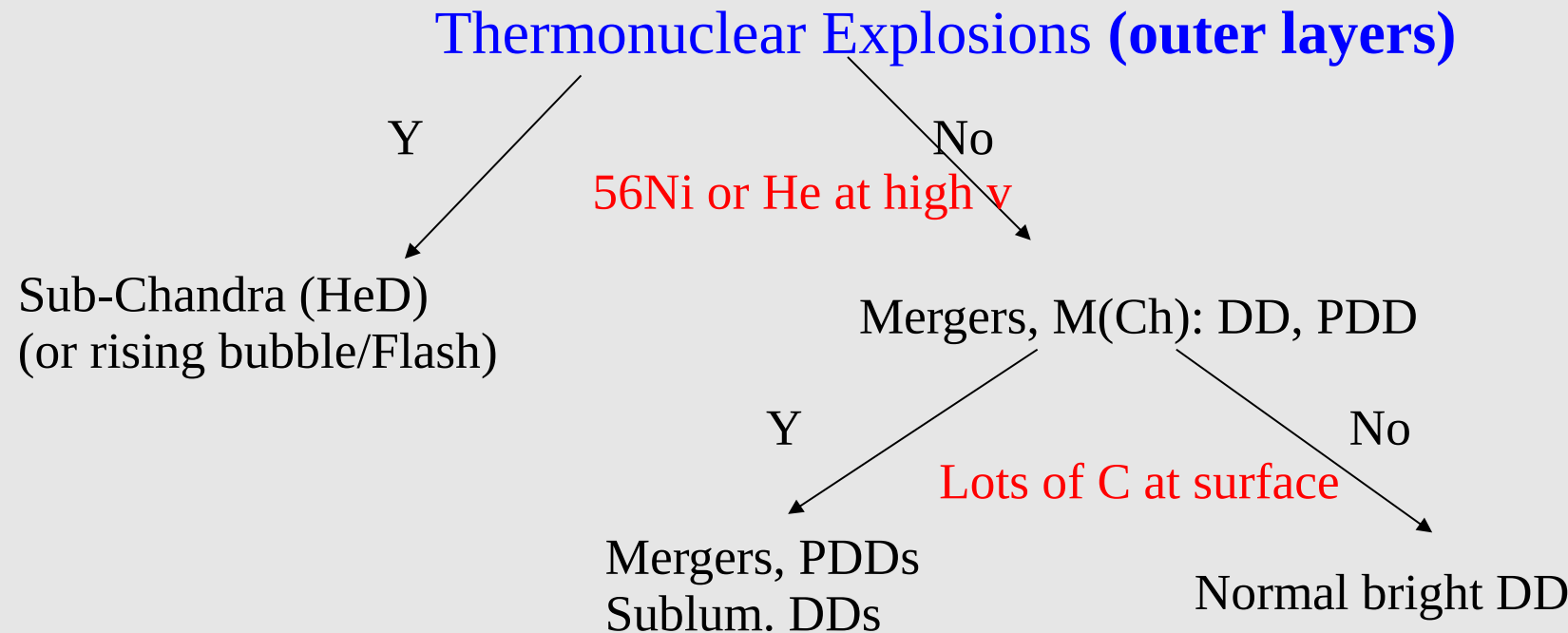
Example: Delayed detonation models for various transition densities $\rho(\text{tr})$

[$M(\text{MS}) = 3 \text{ Mo}$; $Z = 1.\text{E-}3$ solar; $\rho(c) = 2\text{E}9 \text{ g/ccm}$ with $\rho(\text{tr})=8, 16, 25 \text{ g/ccm}$]

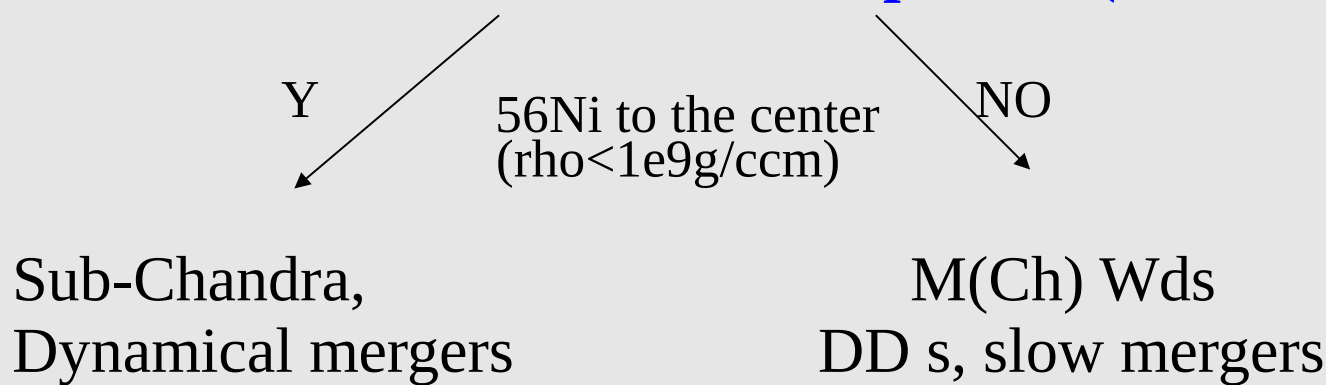


Qualitative difference between spherical scenarios:

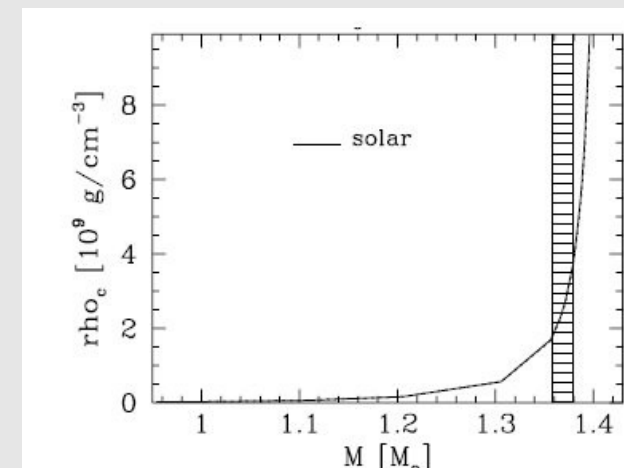
Summary of Generic Chemical Structure (simplified)



Thermonuclear Explosion (inner layers)



COMPLICATION: Mixing (needs to be measured)

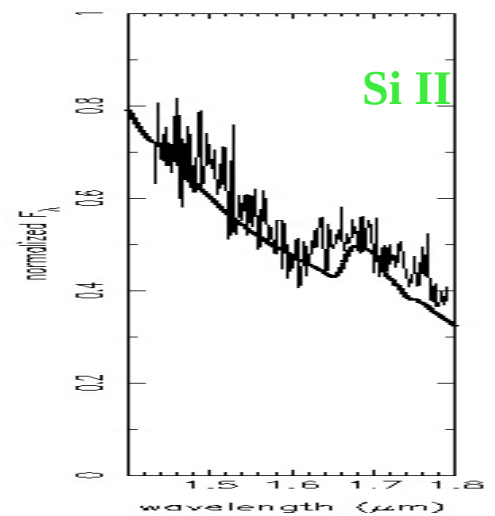
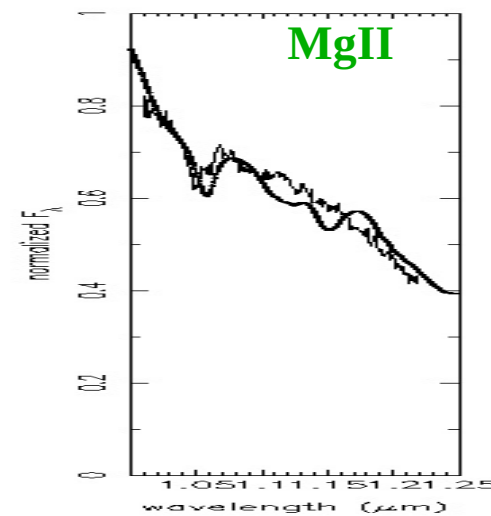
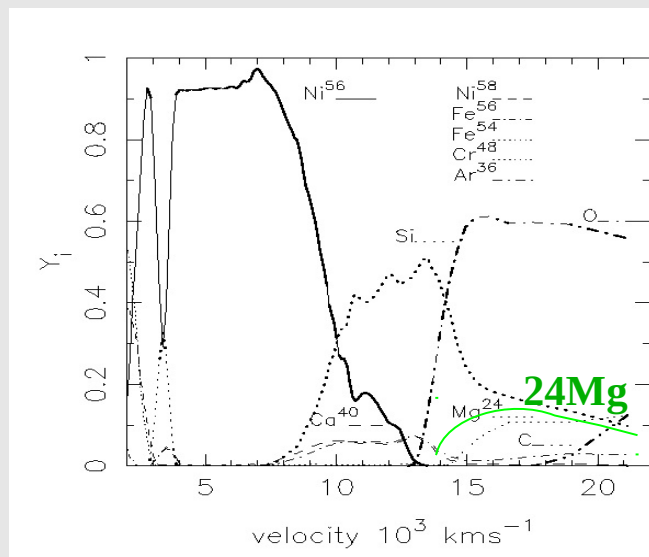


I) Pre-max IR spectra as probes of explosive C & O burning

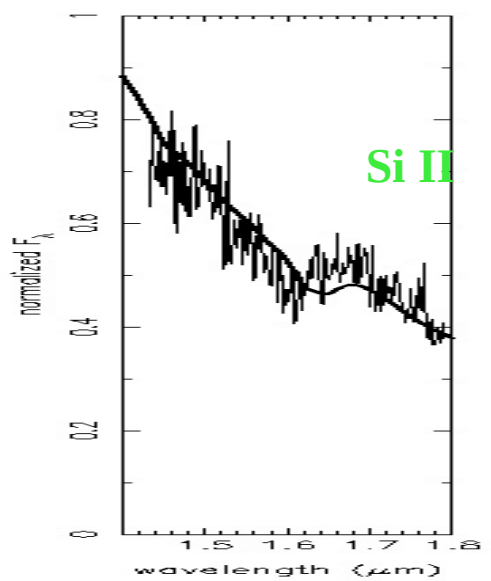
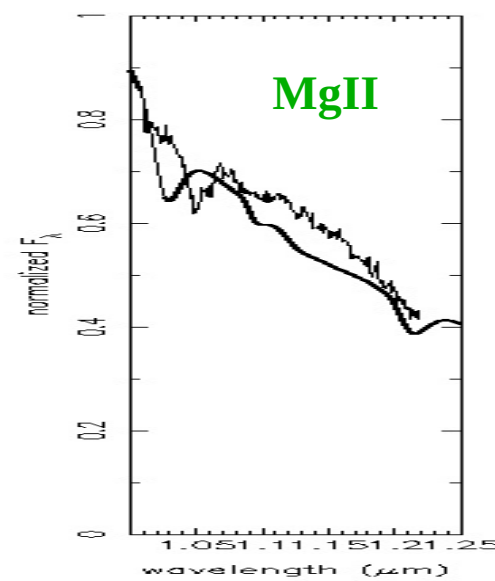
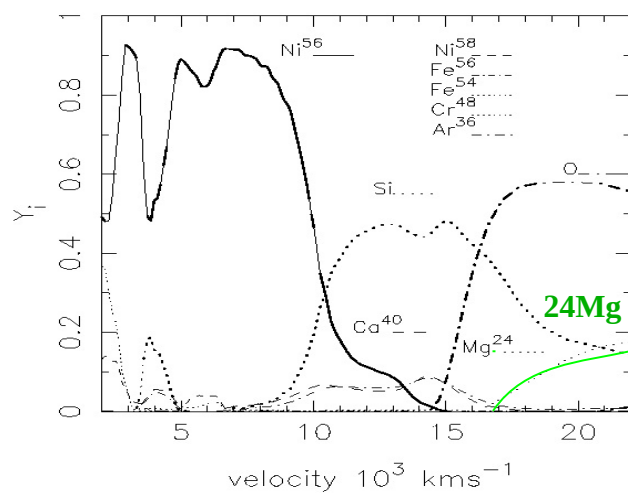
Examples: DD with $\rho(c)=2.5 \text{E}9 \text{ g/ccm}$ & Peter Meikle (Mr. IR)

a) $\rho(\text{tr})=2.0 \text{E}7 \text{ g/ccm}$

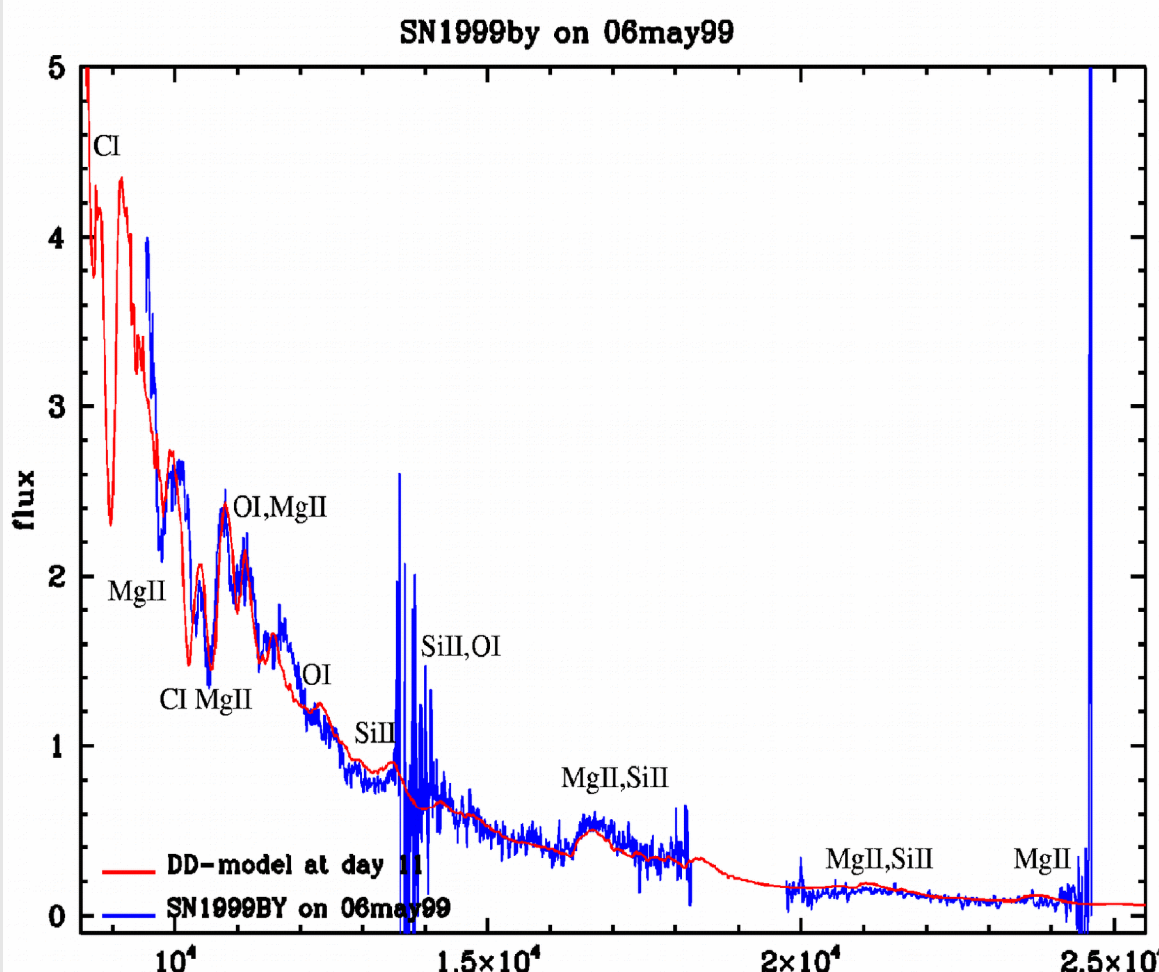
Spectra between 1.05-1.25 & 1.4-1.8 Å



b) $\rho(\text{tr})=2.4 \text{E}7 \text{ g/ccm}$



The nature of subluminous SNels

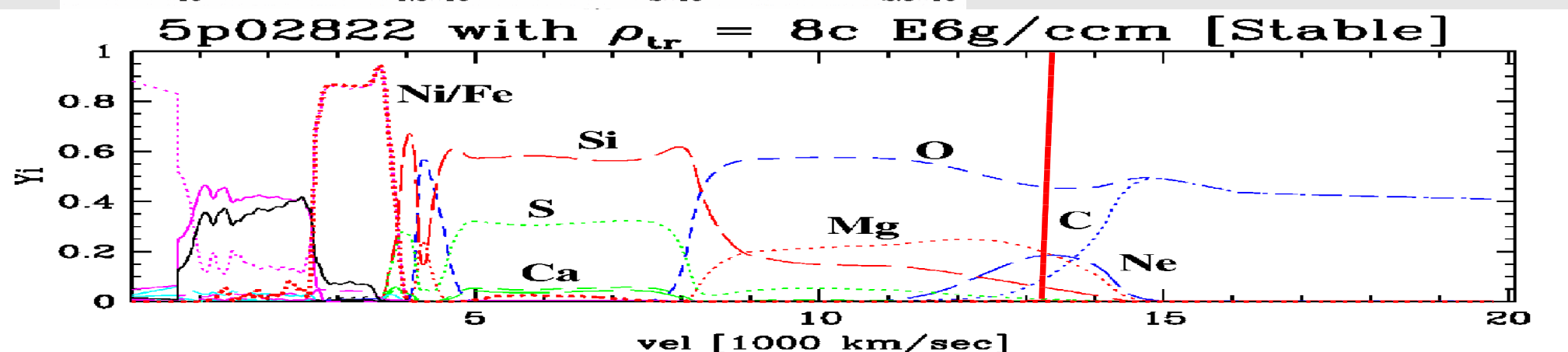


- Spectrum is formed in O-rich layers

model

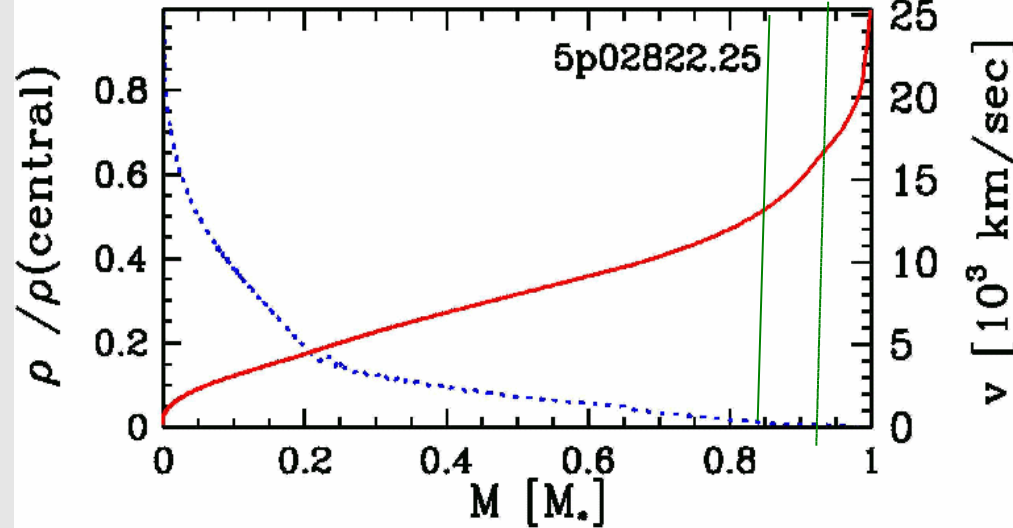
observation

Thompson photosphere

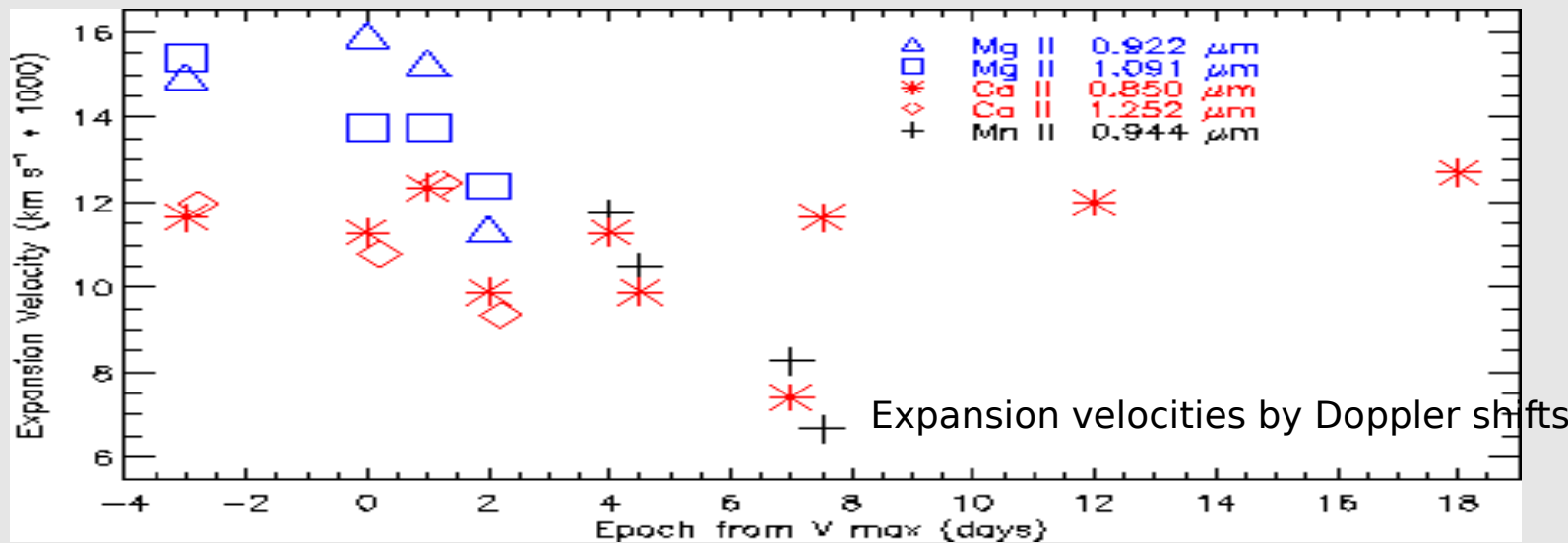
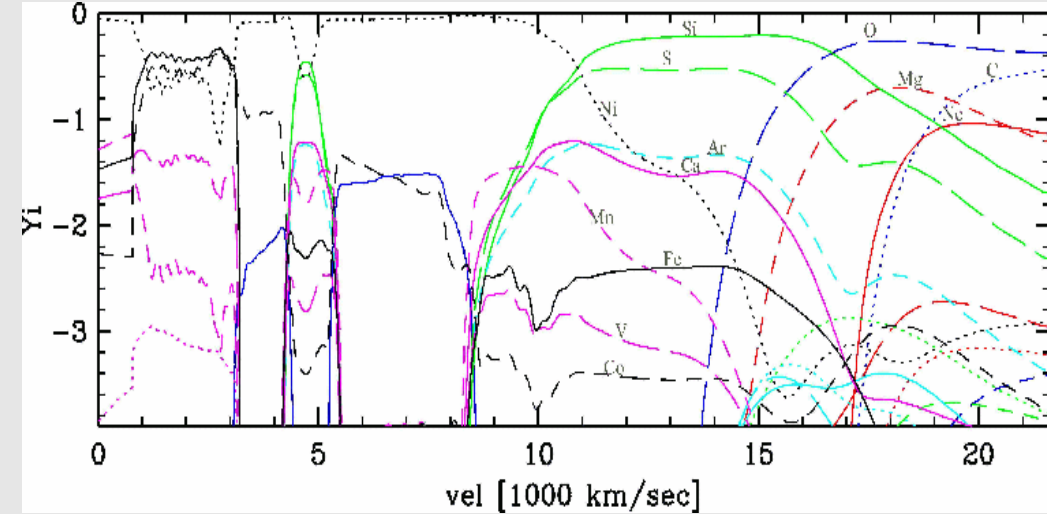


Quantitative Conclusions from the IR-sample

Typical DD model for a normal-bright SN.Ia



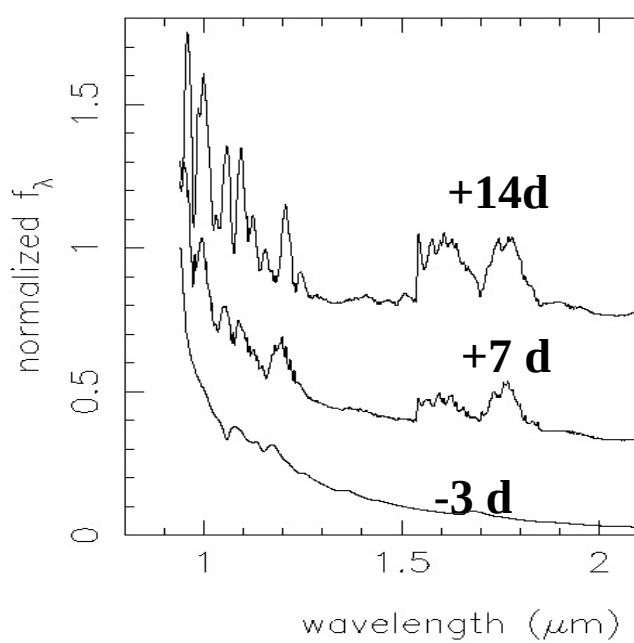
Abundances (log/mass fractions)



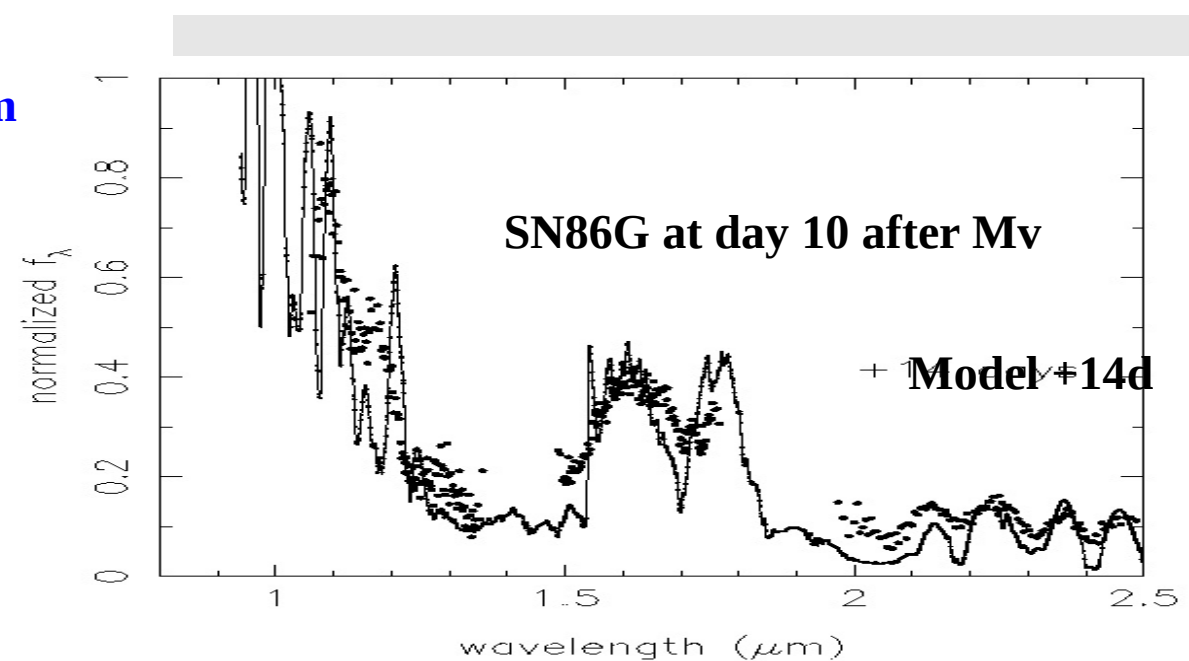
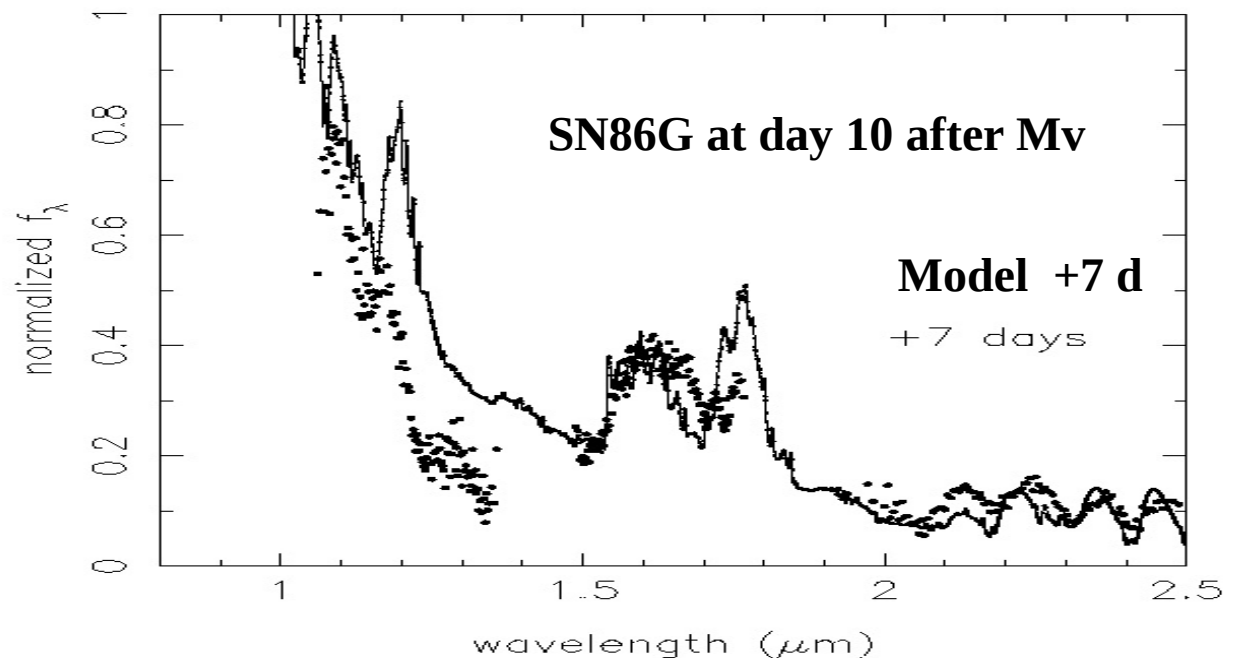
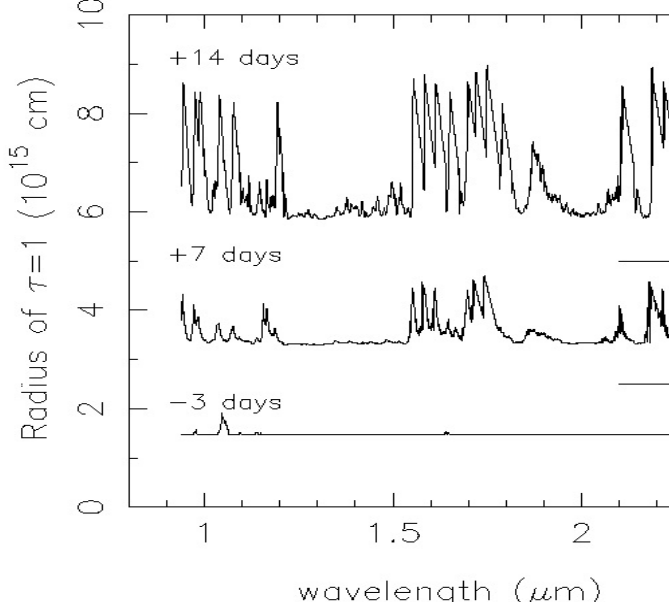
- Mn II is an important probe for the burning temperature in the Si/S region
- Layered, chemical structure (without evidence for non-radial component/mix)
- Minimum Mg II velocities between 12,000 to 16,000 km/sec in the sample
=> typical of unburned matter << 0.1 to 0.2 to Mo !!! (from line wing < 0.1 M_{sun})
- significant individual variations are about 4000 km/sec

II) Post-maximum IR-Spectra of DD200 in Comparison with SN86G

Flux between 1 and 2.5 μ m

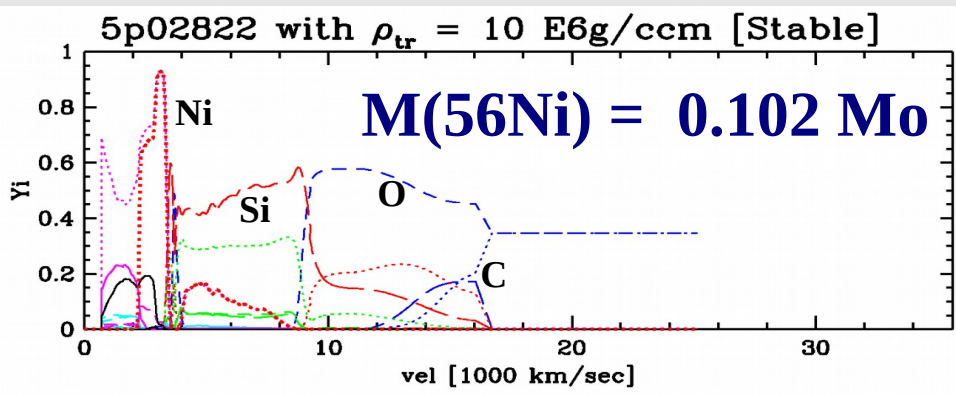


Radius between 1 and 2.5 μ m

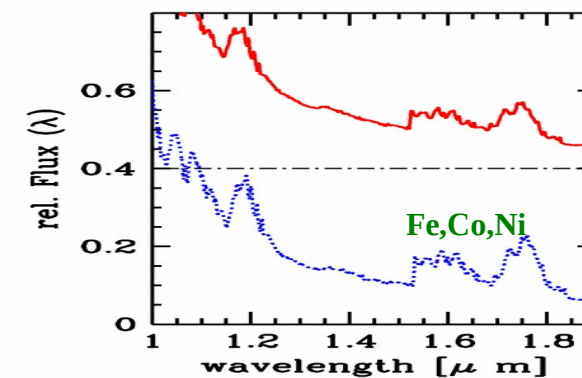
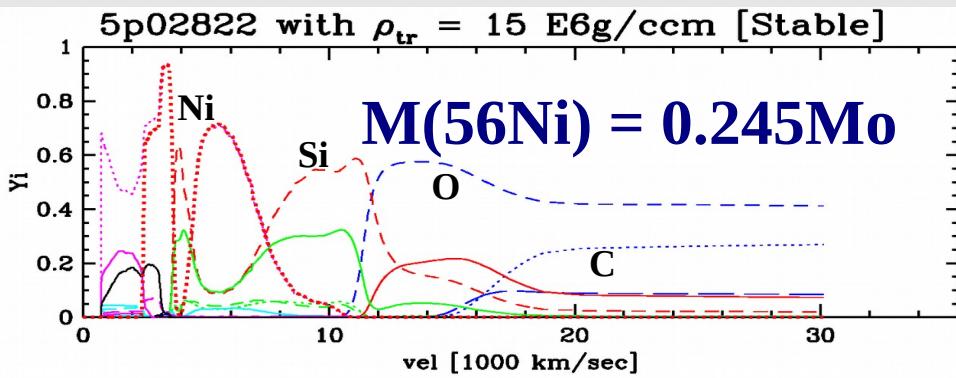
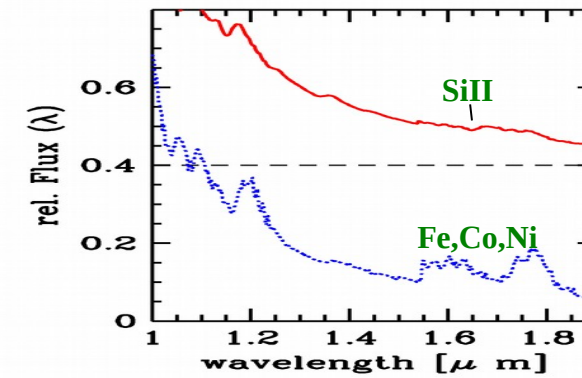


Structures and IR Spectra for Subluminous DD-Models

C/O-WD; $\rho(c) = 2.E9 \text{ g/ccm}$



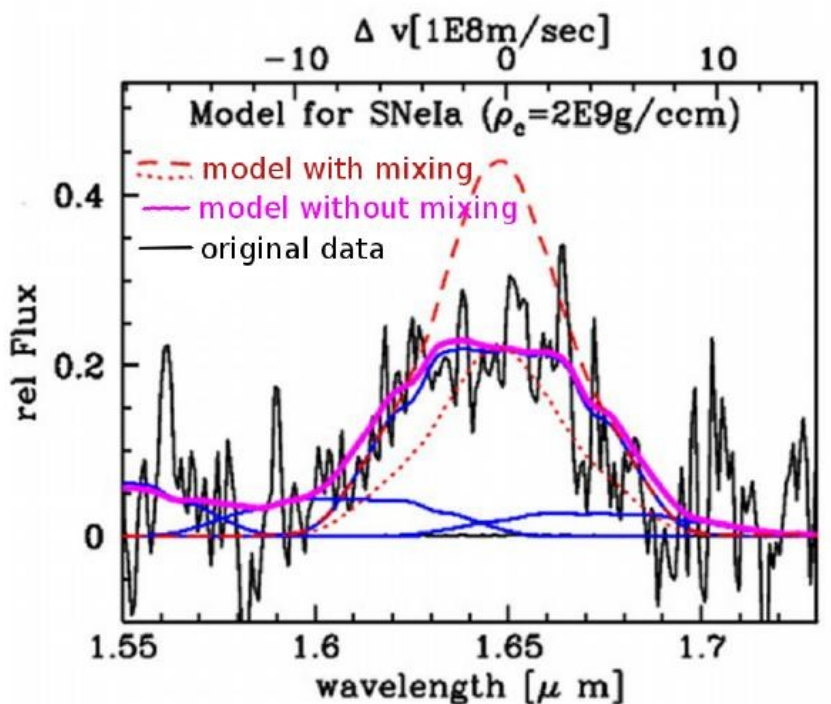
IR-flux 1 & 2 weeks after M(V)



- Iron-island as probe for rising of the H flux (probe of mass above NSE)
- Later rise and lower velocity with decreasing luminosity
- Needed: Spectra or (V-H) LCs

Line Profiles Late-Time NIR Spectra & LCs

Line profiles of late time spectra
 Example: SN2003du at +384d
 (H.etal 2004)



=> $B > 10,000 \dots 1E6 \text{ G} \dots$

(Hetal., 2004,Penny et al. 2014, Diamond 2015)
 $\rho(c) = 2E9 \text{ g/cm}^3$

Remark: [FeII] 1.644 μm is pretty unique

(SN2004hv, Motohara et al. 2006,Maeda et al. 2010)

SN2012Z (Stritzinger et al. 2014)

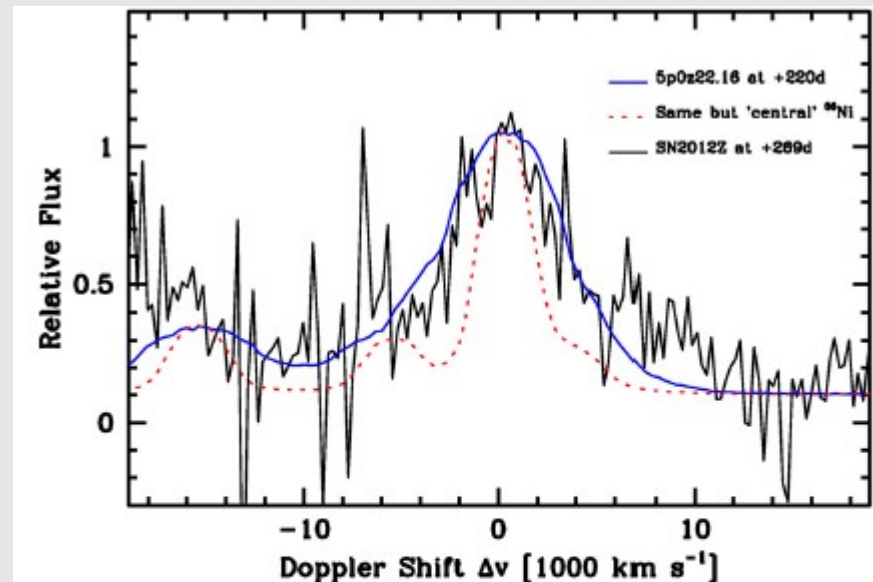
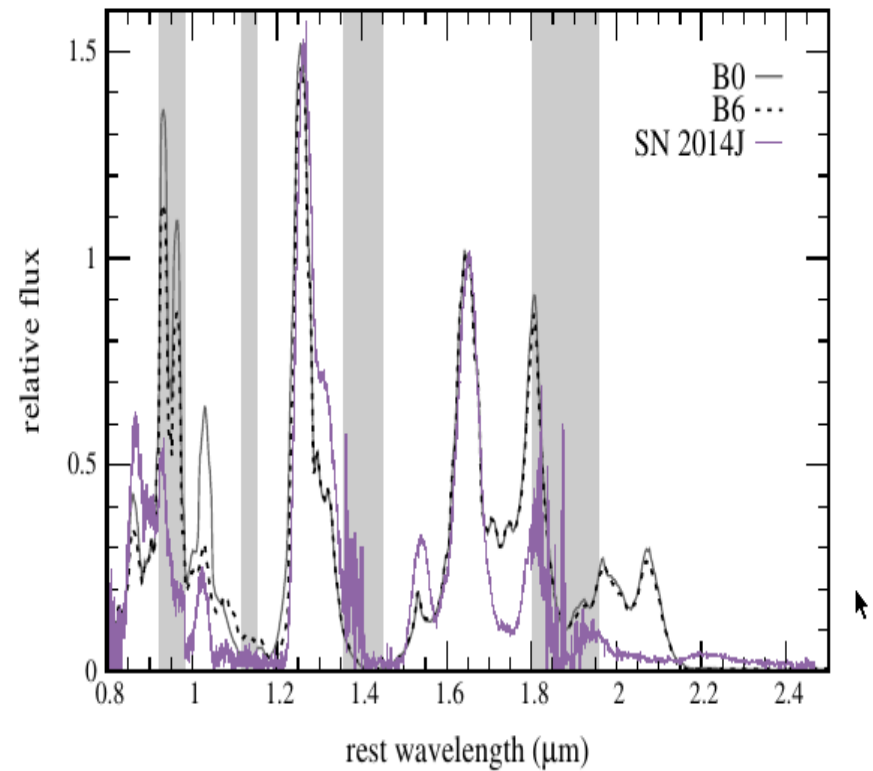
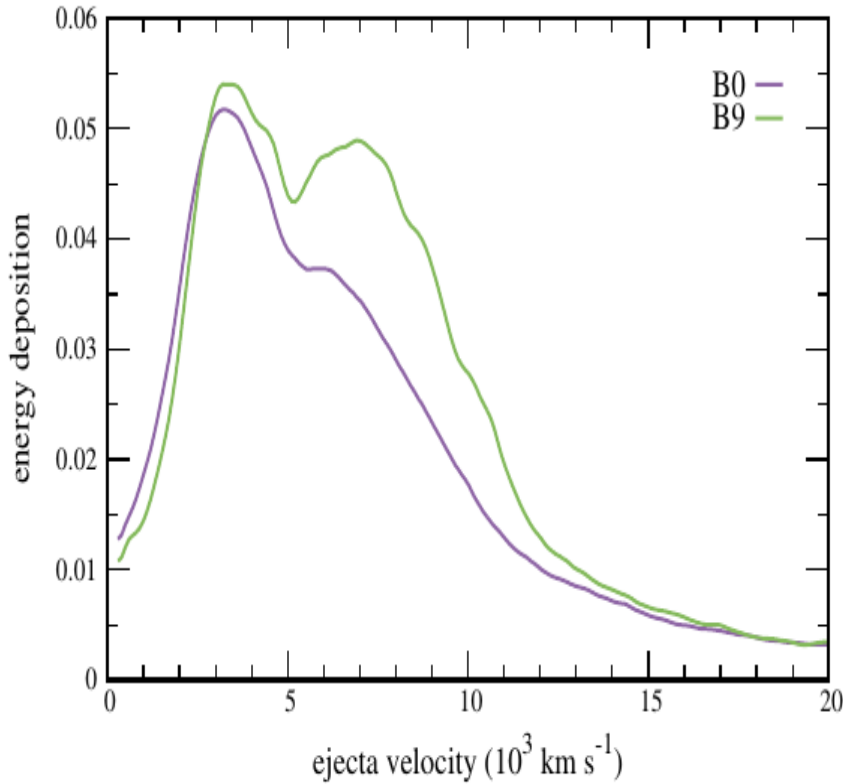


Fig.13. Effect of the ^{56}Ni distribution upon the late phase [FeII] $\lambda 1.64 \mu\text{m}$ feature. Comparison of this feature from the +269d spectrum of SN 2012Z (black) to the expected line profile computed from the 5p0z22.16 model at +220d for two different ^{56}Ni distribution. Plotted in blue is the synthetic spectra for the original model which has a hole in the ^{56}Ni distribution of $\approx 3000 \text{ km s}^{-1}$, while in red is the synthetic spectrum with ^{56}Ni concentrated in the center.

=> Subluminous SNe give narrower lines
 Is this is not always true, or do we need less mass
 (with $L \sim \text{SQRT}(M)$) & no electron capture ?

Probing mixing and positron transport effects in the NIR ?

Diamond et al. 2018: The S II 1.05 mu feature at 466 days in SN2014J

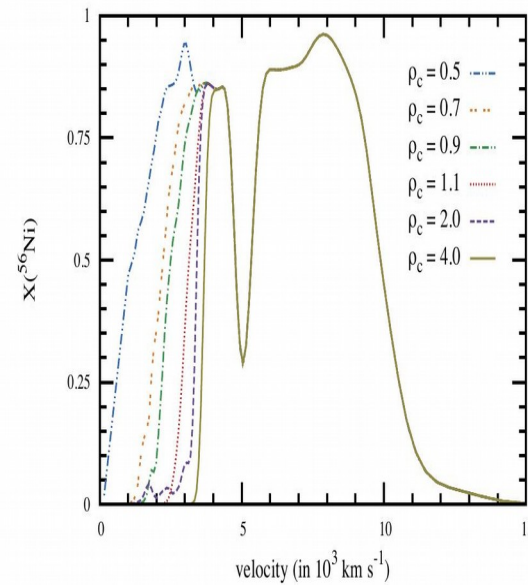


- Non-local excitation of SII by positron transport

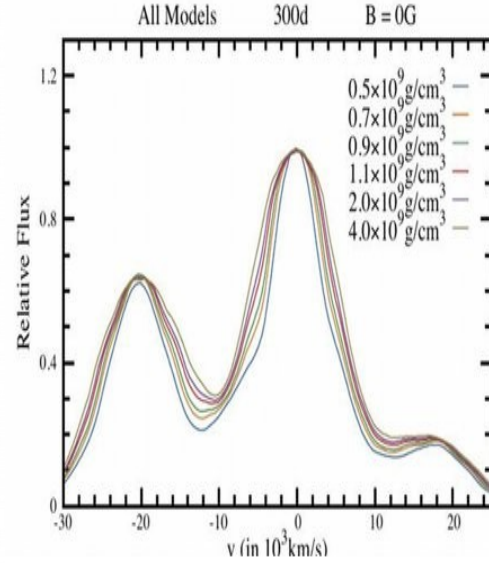
The [Fe II] line at 1.644 mu as “Swiss-Armee Knife” @ SN 2005df

(Diamond et al., 2015, 2017, and see Tiara’s talk)

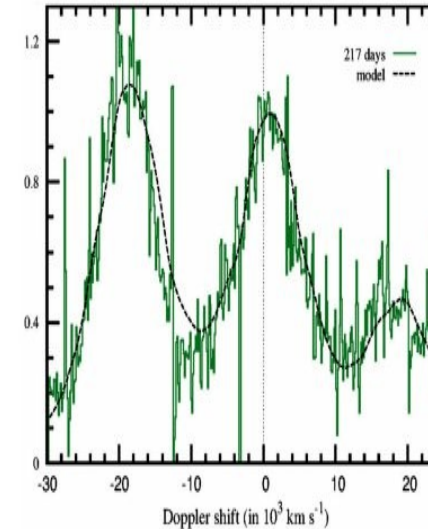
$X(56\text{Ni}) = f(v)$
for $\rho_c(c)$



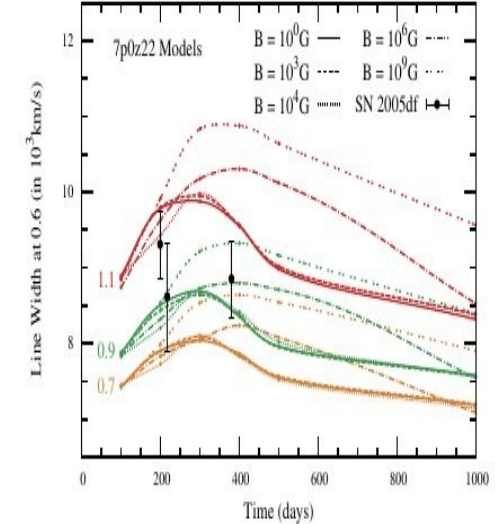
Theoretical Profiles
with Doppler-shift



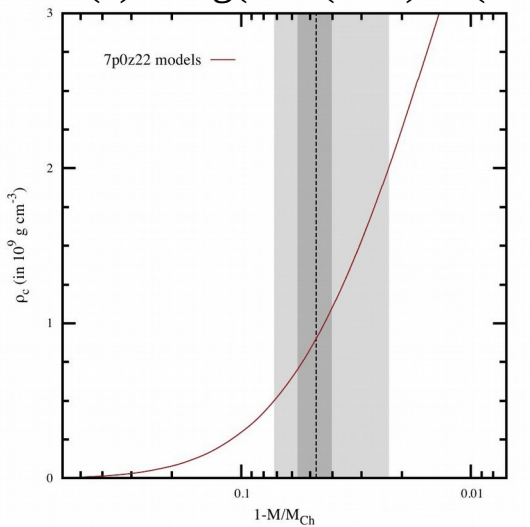
SN05df vs. Model
at day 200



Half width=f(t)
for $B=0, 1\text{E}4$ & $1\text{E}9\text{G}$



$$\rho_c = \log(1 - M(\text{WD}) - M(\text{Ch}))$$



Results for SN 2005df

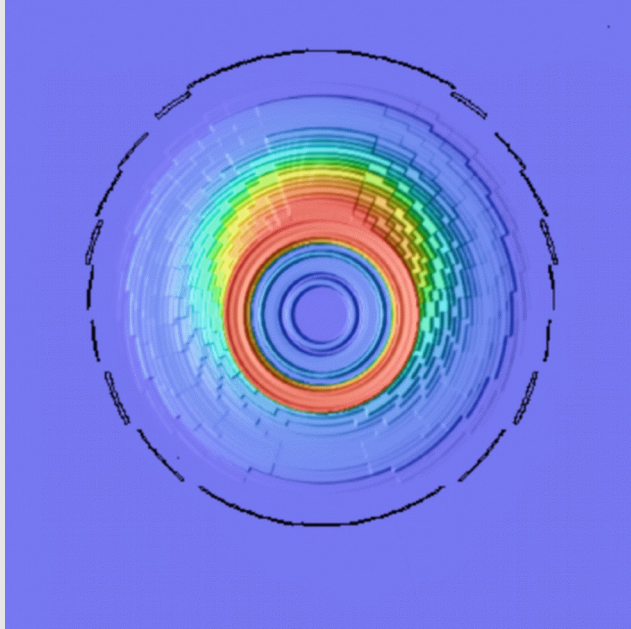
- $M(\text{Ch})$ explosion likely
- $B > 1\text{E}6 \text{ G}$ best but $B=0$ possible (time series is needed)
- low density (almost too low for H accretor
-> He or C (SD or DD progenitor system))

Forward to the past: Search for the off-center DDT?

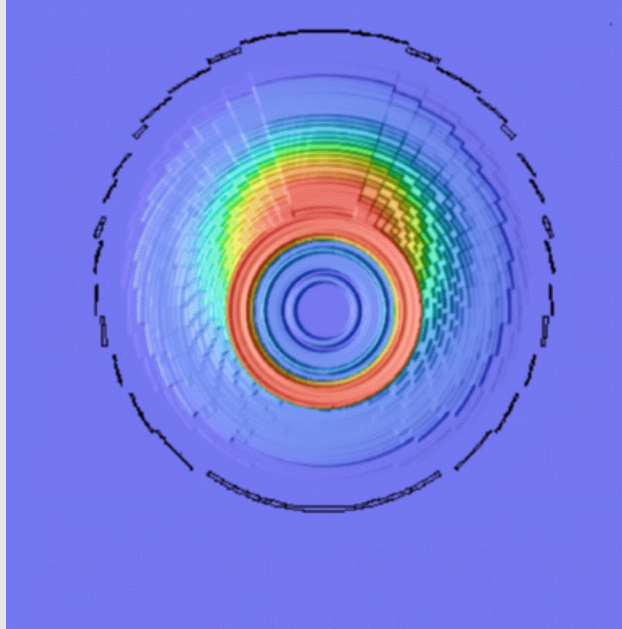
Approach: Spherical deflagration to mimic little mixing and DDT

The ^{56}Ni distribution for various off-center ignitions

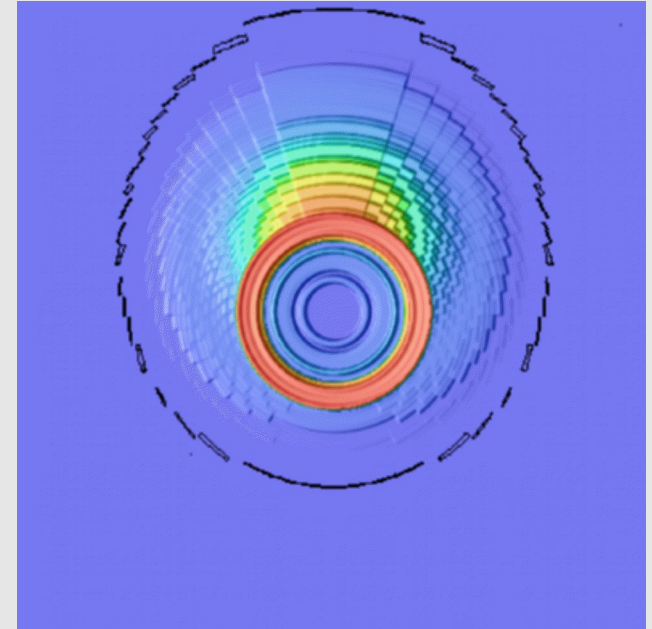
0.1M



0.3M



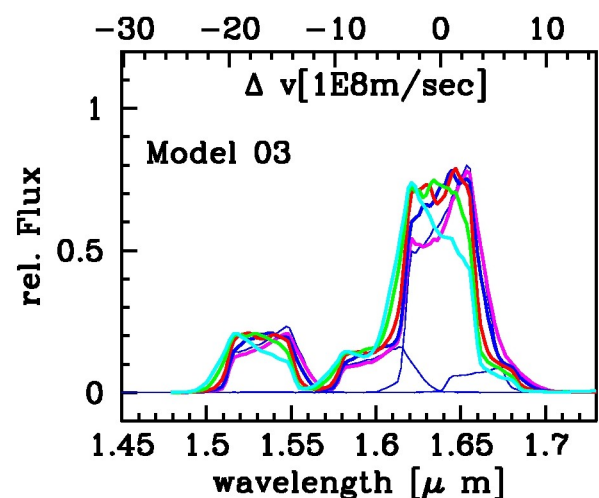
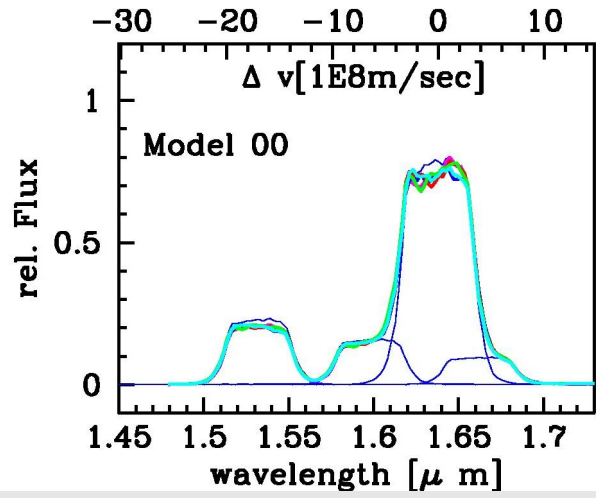
0.9M



- Ni distribution depends on the ignition point
- Asymmetric distributions are caused by 'runtime' effects

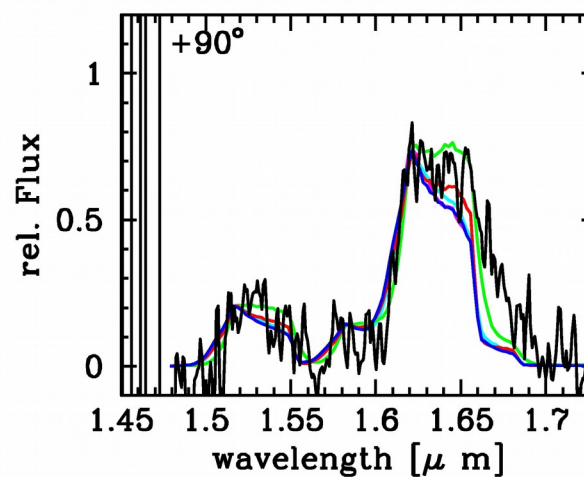
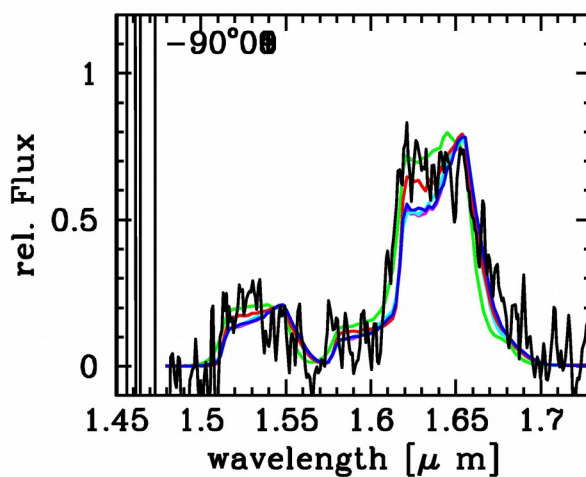
Forward to the past: Search for the off-center DDT?

Approach: spherical deflagration to mimic little mixing and DD



Orientation of observer

- 90°
- 30°
- 0°
- +30°
- +90°



Various models seen from a given angle

- 09
- 05
- 03
- 01
- 00

PROBLEM: non-unique solutions

Asymmetry in profile => seen from -30 to -90 degrees

Still flat topped => -30 degrees are favored for 0.3 off-center

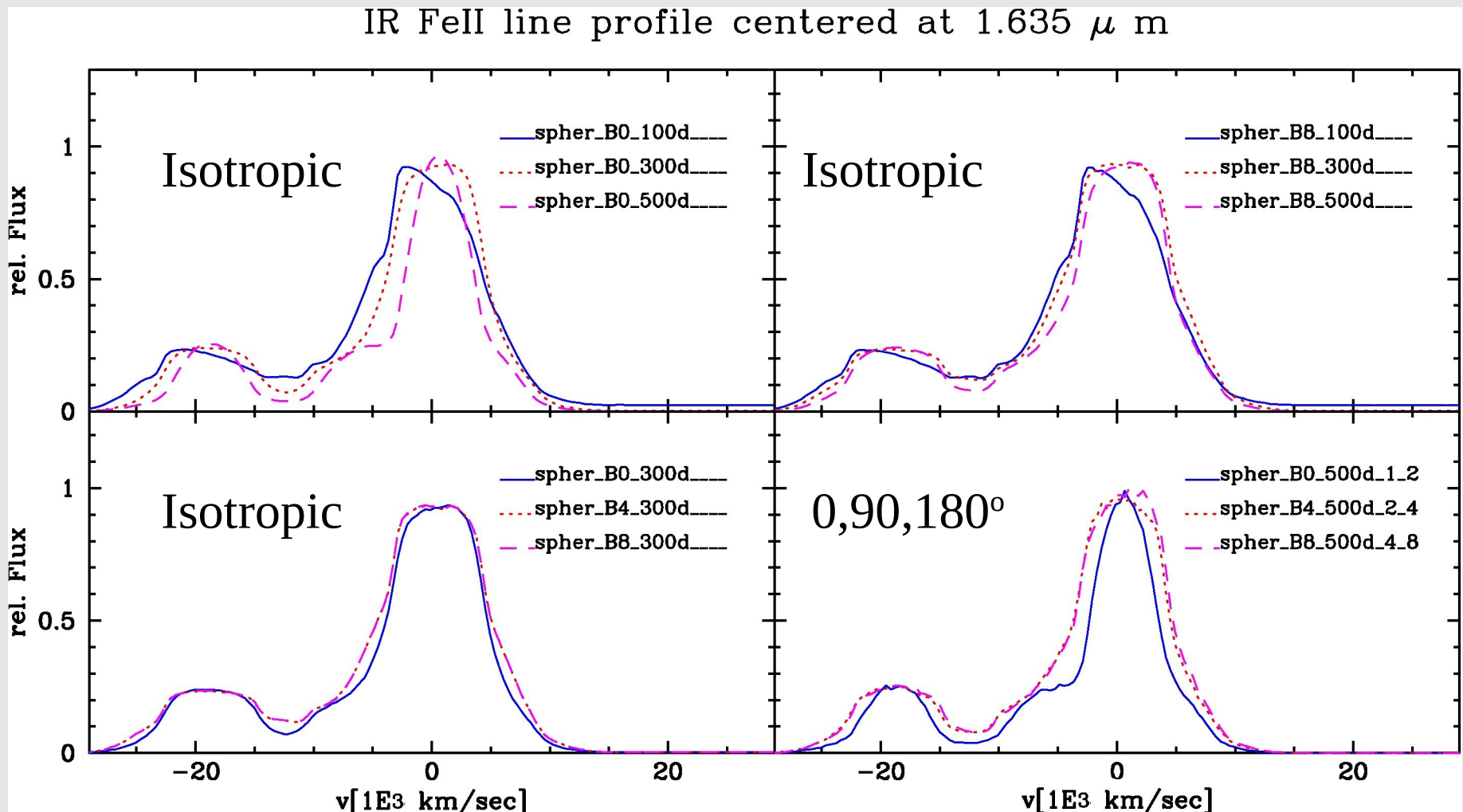
or -90 degrees for 0.9 off-center

Discrepancies => deflagrations not entirely symmetric

Influence of GRT& Positron Transport Effect of Magnetic Fields & Clumps

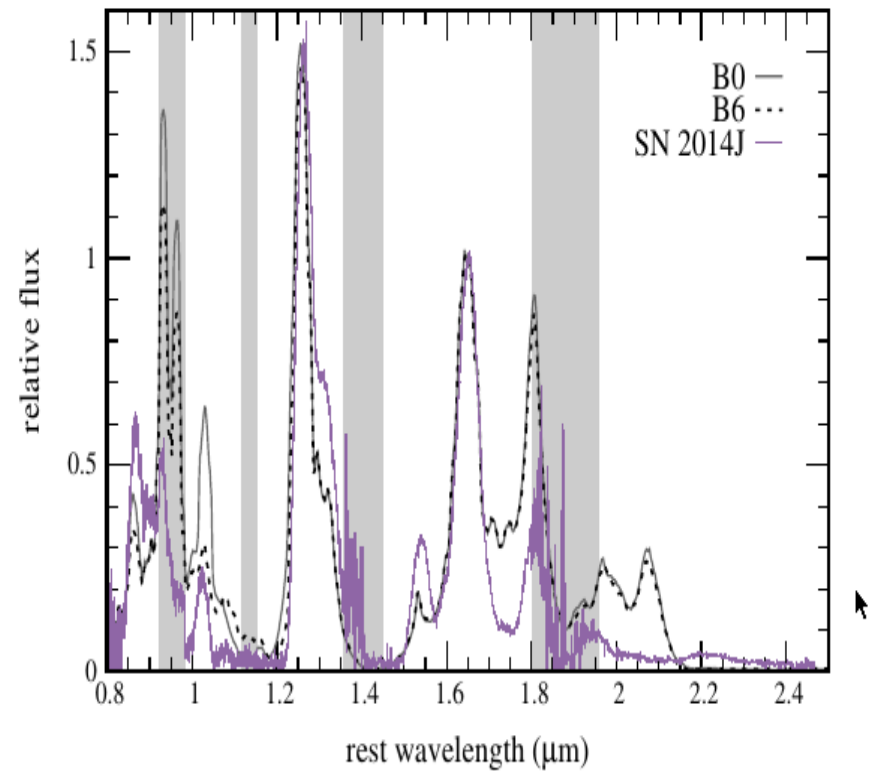
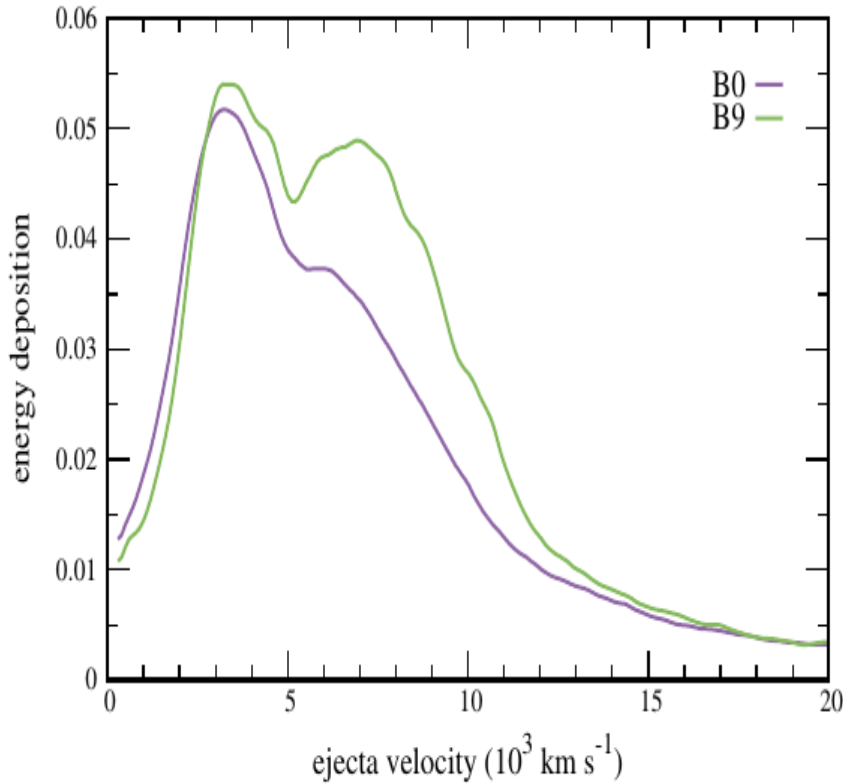
(Penny & H. 2015)

Example: Effect of a large scale dipole field on isolated Co lines



Probing mixing and positron transport effects in the NIR ?

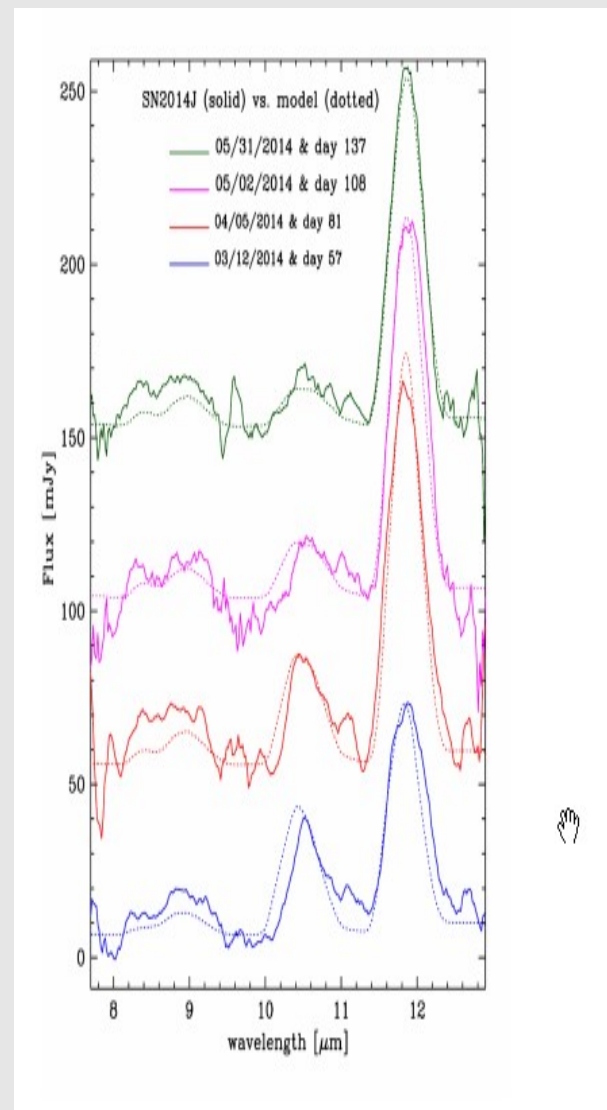
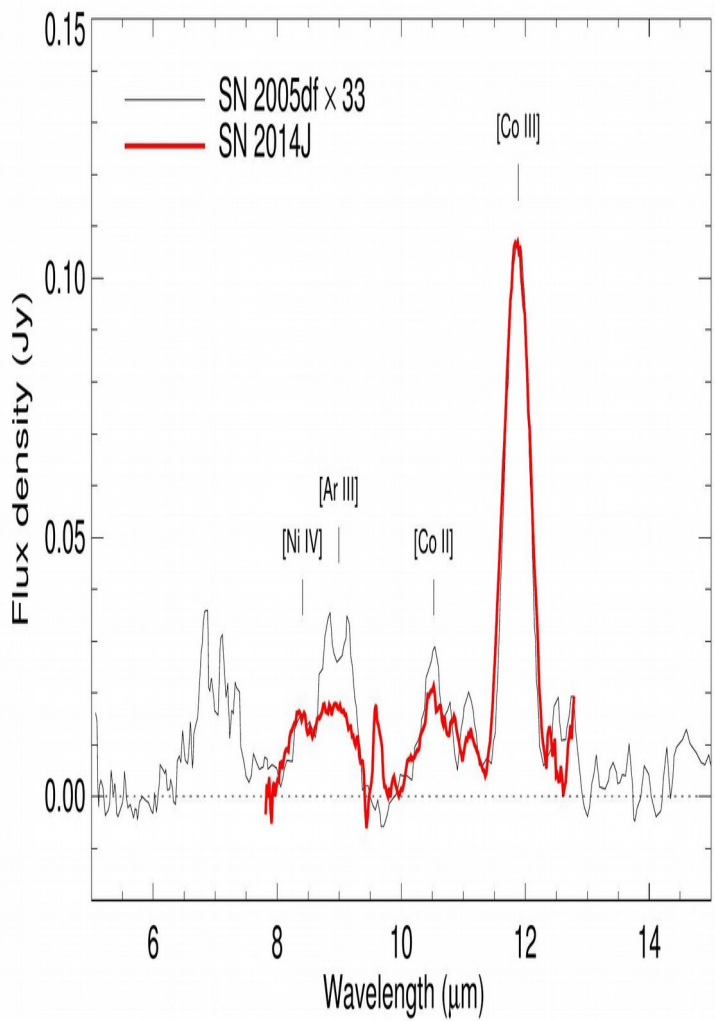
Diamond et al. 2018: The S II 1.05 mu feature at 466 days in SN2014J



- Non-local excitation of SII by positron transport

Why do we need Mid-IR spectra ?

SN 2014J and SN2005df have the same M(V), dm15, [Co III]
but differ in the Ar distribution and, definitely, no Chromium.
(Telesco et al., 2015)



Others:

- Direct measure of photon redistribution
- [Co III] @ 11.8 μm as new standard candle ?
- magnetic fields
- mixing ...

Diamond et al. 2017

How can we get ^{57}Co in all the mess

Questions:

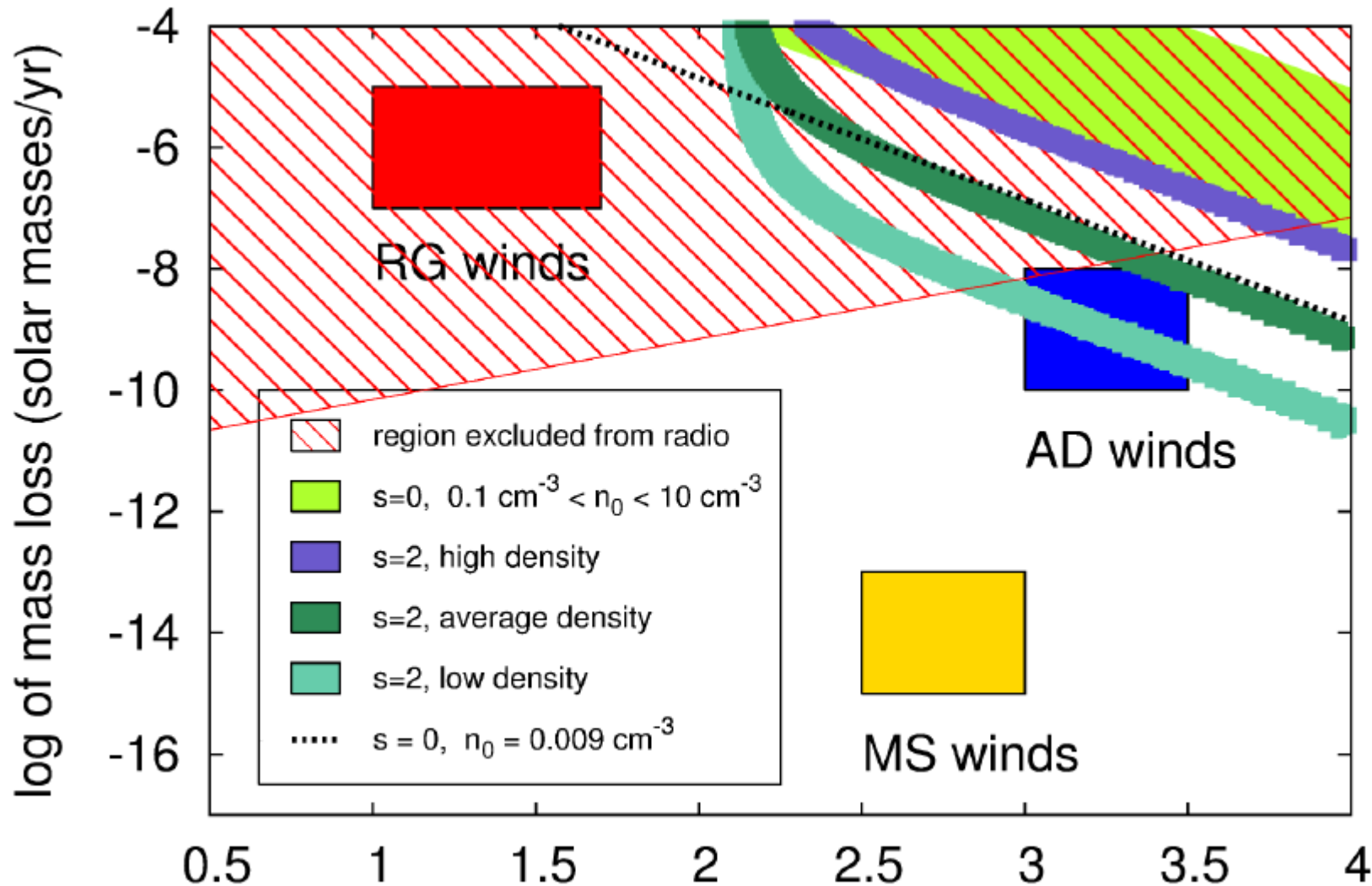
- progenitor link (see other talks)
- diversity, mixing, B-fields

Wishlist for IR:

- Early time spectra & LCs with 3 days latency (C,He,Mg, ...)
- Post maximum spectra or V-H
- NIR and MIR line profiles between 200+ days
- **Important:** Supporting observations for the same objects

Constraints from X-ray, radio and narrow absorption lines

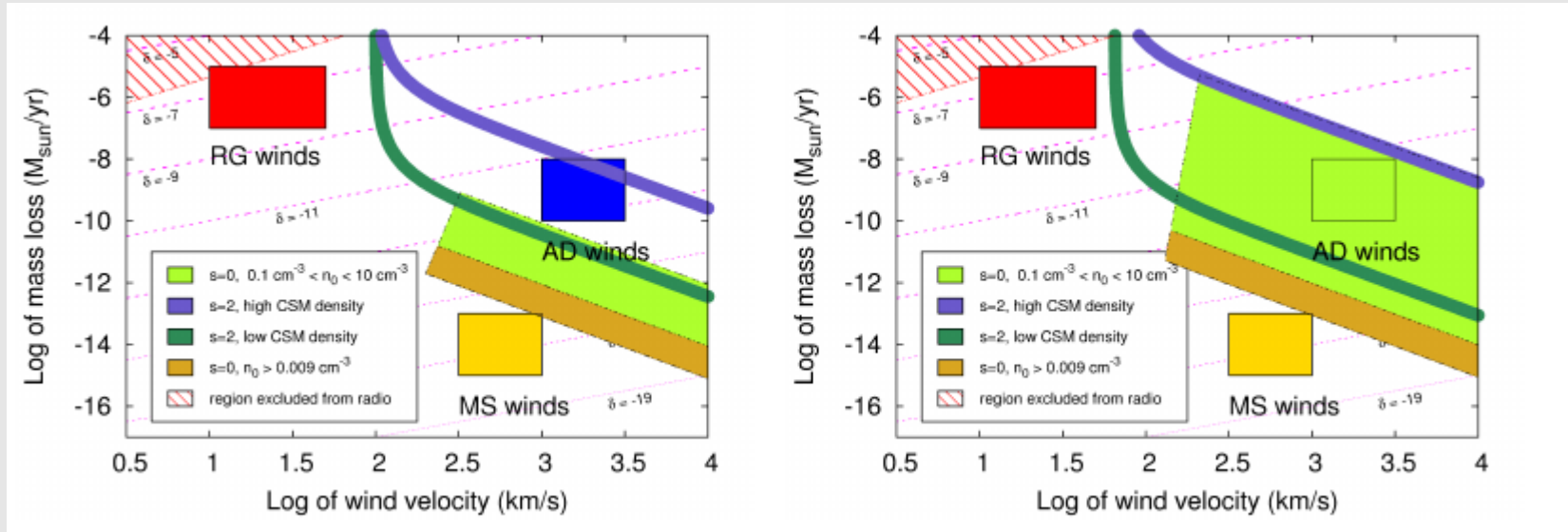
Example SN2014J (data from Margutti et al. 2012, Phillips et al. 2012)



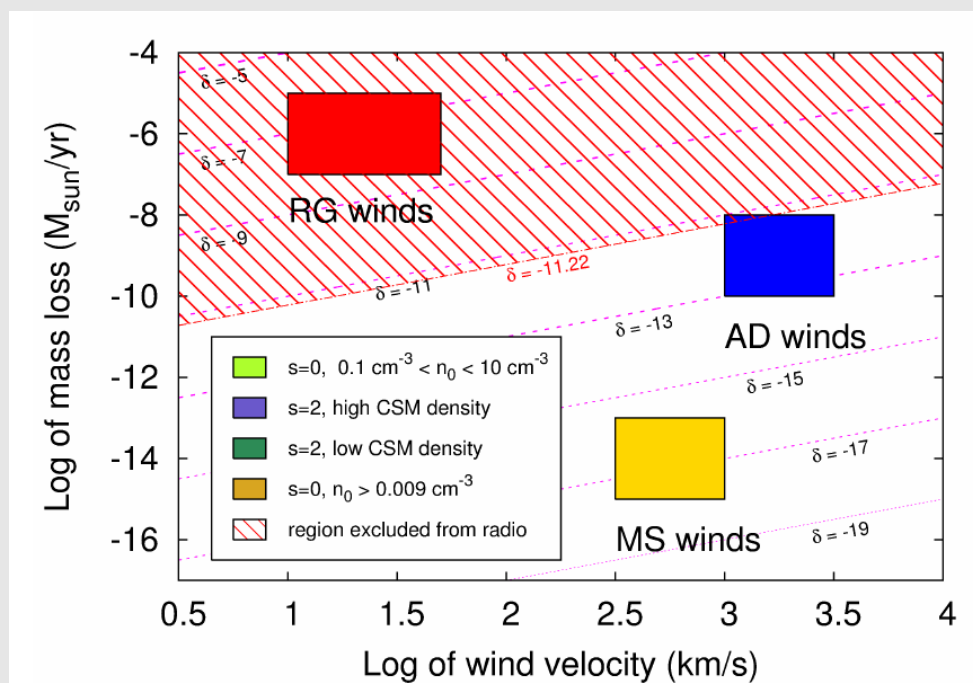
→ Consistent with accretion disk wind (1E-8 Mo/yr and 1000km/sec) running into Constant density (0.008 particles/ccm)
Stellar winds ($M/\text{yr}, v(\text{progenitor wind})$) = $(1\text{E-7}, 60)$ & $(1\text{E-5}, 20)$

Constraints from X-ray, radio and narrow absorption lines

Example SN PTF 11lx (with 2 shells suggested by Dilday et al. 2012)



SN2011fe:



limit from radio by
Chomiuk et al. 2012